Applied Catalysis A, General 698 (2025) 120234

Contents lists available at ScienceDirect

Applied Catalysis A, General

journal homepage: www.elsevier.com/locate/apcata

One step erythritol hydrodeoxygenation towards green butadiene over mixed molybdenum-rhenium supported catalysts

G. Ioannidou [a], M. Drexler [b], U. Arnold [b], J. Sauer [b], A.A. Lemonidou [a,c,*]

[a] Department of Chemical Engineering, Aristotle University of Thessaloniki, University Campus, Thessaloniki 54124, Greece
[b] Karlsruhe Institute of Technology (KIT), Institute of Catalysis Research and Technology (IKFT), Hermann-von-Helmholtz-Platz 1, Eggenstein-Leopoldshafen, 76344, Germany
[c] Chemical Process & Energy Resources Institute, Centre for Research and Technology-Hellas, Thessaloniki, 57001, Greece

ARTICLE INFO

Keywords:
Erythritol
Catalytic hydrodeoxygenation
Rhenium
Molybdenum
Butadiene

ABSTRACT

This work explores the one-step catalytic process of erythritol hydrodeoxygenation (HDO) to 1,3-butadiene over supported Re and mixed Mo-Re oxides on carbon black. Catalyst screening under reducing H_2 atmosphere was performed in liquid phase under batch conditions. Mixed Mo-Re catalysts show the best HDO performance, as they are active towards C-O scission with mild hydrogenation activity, contributing to preservation of the C=C bond of 1,3-butadiene. The effect of reaction parameters was exploited over the promising 5Mo-10Re/CB catalyst. 3-butene-1,2-diol is the main intermediate to 1,3-butadiene formed at short reaction times while longer reaction times lead to butenes. Maximum 1,3-butadiene selectivity 93 % was achieved at 51 % erythritol conversion at 140 °C, 60 bar and 5 h reaction time. XPS measurements of fresh and used materials indicated that the upper surface layer consists of fully and partially reduced Mo and Re species, which according to CH_3OH-TPSR host both redox and acid sites.

1. Introduction

The exorbitant use of fossil resources, mostly for energy production, has a negative impact on the environment, thus leading to the risk of climate breakdown [1]. Fossil feedstocks, the current dominant resource of energy production, as well as of chemicals, are the main contributors to greenhouse gas (GHG) emissions, significantly contributing to climate change [2,3]. Chemical industry, which is the industrial backbone of many developed countries, is a very large energy consumer emitting between 1.5 and 2 billion metric tons of CO_2 per year [4,5]. Among the different chemical feedstocks, light C_2-C_4 olefins are considered the key building blocks of chemical industry, and their production is responsible for releasing around 400 million metric tons of CO_2 per year [5], as it is highly depending on fossil-based technologies (naphtha steam cracking, fluid catalytic cracking). The global olefin market demand has dramatically increased as they can find applications in a wide product spectrum, such as polymers, plastics, synthetic rubbers, packaging, and others [6], while their production is projected to raise USD 329.20 billions by 2028 [7].

The C_4 olefins, such as 1,3-butadiene (BD), butenes, butylene, are the third most important olefins following ethylene and propylene. Among them, 1,3-butadiene is of greatest importance in polymer chemistry, the production of which is primarily driven by the demand for rubbers (polybutadiene, styrene-butadiene) which can be used for the production of tires [8]. The majority of its production (95 %) originates as by-product of ethylene production through steam cracking, while only a small amount stems from n-butane dehydrogenation [9]. However, even though the latter process seems to be very promising compared to the former [10], it still lies ahead in terms of thermodynamic limitations due to its high endothermicity [11]. The most important remark that cannot be addressed is the sustainability aspects of the process as the origin of the feedstock is still derived from fossil fuels.

With the chemical industry facing the decarbonization challenge, the development of new technologies to reach net-zero CO_2 emissions for producing both chemicals and fuels has become indispensable. To achieve this, carbon-neutral resources are required [4]. Biomass (e.g. lignocellulosic) and its derivates (e.g. polyols) are considered auspicious and environmentally friendly feedstocks that can be used to face this challenge due to their carbon-neutral footprint [12–15]. Biomass derived polyols, such as glycerol, erythritol, sorbitol, xylitol etc., portray an alternative and promising resource for producing sustainable olefinic compounds, as well as important chemicals and fuels. However, their

* Corresponding author at: Department of Chemical Engineering, Aristotle University of Thessaloniki, University Campus, Thessaloniki 54124, Greece.
E-mail address: alemonidou@cheng.auth.gr (A.A. Lemonidou).

https://doi.org/10.1016/j.apcata.2025.120234
Received 3 October 2024; Received in revised form 19 March 2025; Accepted 20 March 2025
Available online 23 March 2025

highly oxygenated functionality prevents their direct use and thus the C-O bond scission or substitution is of outmost importance [16–18]. Different catalytic processes, namely hydrogenolysis, dehydration, decarbonylation etc., have been reported/applied over the years to achieve oxygen removal. Among them, hydrodeoxygenation (HDO) is the most encouraging and effective one to accomplish oxygen removal in H_2 reductive atmosphere, especially when hydrocarbons are the target product [19,20]. Several types of HDO catalysts have been reported over the years, such as precious metals (e.g. Re, Ru, Rh), non-precious metals (Ni, Cu, Fe), transition metal oxides (Mo, W) and/or mixed metal catalysts [21–25].

Erythritol, a C_4 sugar alcohol, is a low-calory and non-glycaemic sweetener mostly used in food industry. It is the first polyol which has been industrially produced through fermentation processes [26,27]. The worldwide production of erythritol equals to 60.000 t/year with its price being comparable to other fermentation products. Although it has not been considered as a platform chemical compared to other sugar alcohols, namely glycerol and sorbitol, its potential use as raw material to produce useful chemicals within the concept of a biomass refinery has recently started to attract the scientific interest. Erythritol can be converted to important chemicals, such as 1,4-anhydroerythritol, butanediols and others via various catalytic processes [28]. Catalytic hydrodeoxygenation (HDO) of erythritol is a challenging and alternative path to manufacture 1,3-butadiene. The choice of the catalytic material is of farthest importance, as a notable number of products can be formed, (Scheme 1) based also on the reaction conditions. Targeting 1, 3-butadiene production, the catalyst should be active towards C-O scission maintaining the 4 C-atoms erythritol backbone. In most cases, the selection of the catalytic material can be made based on similar reactions of other polyols, such as glycerol [22,29,30].

To the best of our knowledge, the available reports in the open literature regarding erythritol HDO towards 1,3-butadiene are very scarce, especially with the use of heterogeneous catalysts. The reported studies involve the use of homogeneous Re (CH_3ReO_3) and Ru ($RuBr_3$) catalysts using mostly alcohols as reducing agent [29,31,32]. There is only one comprehensive work by Tomishige and coworkers employing heterogeneous catalysts, more specifically cerium-supported rhenium catalysts [23,33]. They first studied the effect of Re mixed with Au catalysts for HDO reaction of glycerol using H_2 as a reducing agent. They found that Au particles with 10 nm size in ReO_x-Au/CeO_2 are effective candidates for retaining the C=C bond of allyl alcohol during glycerol HDO experiments and they further applied this catalyst on erythritol HDO and achieved 81 % yield of 1,3-butadiene. Afterwards, the same group extensively studied 1,3-butadiene production from erythritol over ceria-supported rhenium catalysts modified with metals, such as Ag, Cu, Pd, Ru, Ni and Ir. It was found that the ReO_x-Ag/CeO_2 catalyst exhibits the highest selectivity towards 1,3-butadiene, achieving a maximum of 86 % yield for complete conversion of 5 wt% erythritol in 1,4-dioxane under batch conditions at 8 MPa H_2, 140 °C and 20 h. Under these conditions, butenediols were the main byproducts detected. By further exploring the reaction pathway, it was proposed that the reaction proceeds through 3-butene-1,2-diol formation, which is considered as the main intermediate. Although they mentioned that 1,3-butadiene is produced via butenediols HDO, generally according to Scheme 1, its production from butanediols cannot be excluded and thus this route is also included. In addition to catalytically converting erythritol to 1, 3-butadiene, Ota et al. [34] studied the HDO reaction of 1,4-anhydroerythritol to tetrahydrofuran (THF) by testing various combinations of metals (Mo, Re) with Pd, as well as mixed Re-M where M: Co, Ni, Cu, Ru, Rh, Pd, Ir, catalytic materials supported on CeO_2. The results pointed the promising performance of ReOx species and more specifically that of mixed ReOx-Pd/CeO_2 due to its high activity during HDO reaction. It was suggested that the monomeric Re species are the active sites for the reaction. The authors also tested the effect of solvent by employing various solvents such as 1,4-dioxane, dodecane, pentanols, water and 1, 2-dimethoxyethane. The reaction rate was lower in the presence of water, while the higher activity and selectivity was obtained over 1, 4-dioxane. Very recently, Cao et al.[35] investigated the reaction kinetics of erythritol deoxydehydration and hydrogenation of erythritol to butanediols and n-butane in the presence of ReOx-Pd/CeO_2. DFT calculations and in-depth characterization of the materials indicated that catalyst deactivation occurred due to the presence of aggregated ReOx species rather than carbon deposition.

In a previous research study of our group, the catalytic HDO of bioglycerol to propylene in reducing H_2 atmosphere has been extensively studied under both batch and continuous flow conditions [36–39]. The results are very promising, as high propylene yields (60–70 %) were achieved for almost complete conversion at 280 °C and 60 bar system pressure, highlighting the potential use of molybdenum-based catalysts towards 1,3-butadiene formation through

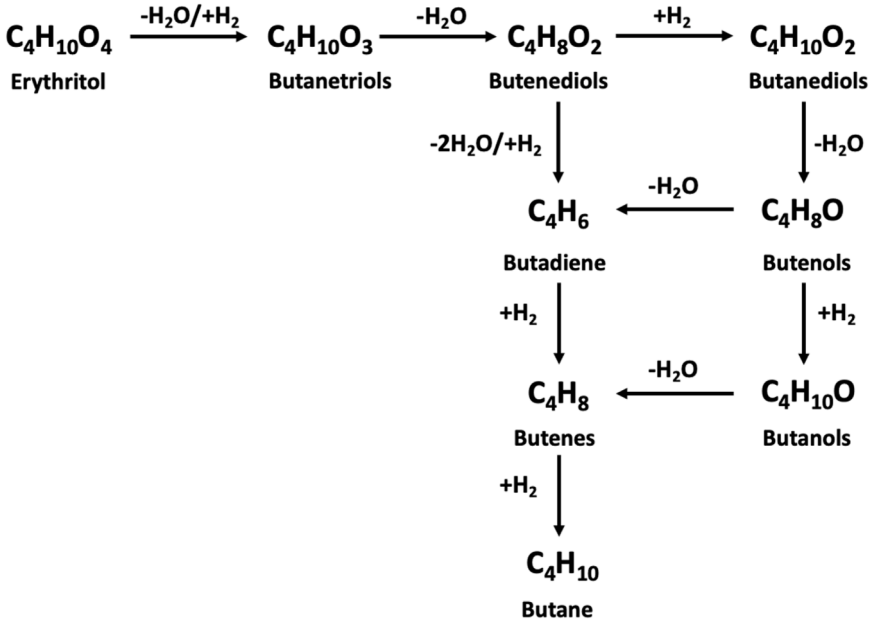

Scheme 1. Potential reaction network and product distribution of erythritol conversion.

erythritol HDO. In addition, considering the limited available reports, heterogeneous catalysts based on transition metal oxides (W) having similar properties with molybdenum, as well as rhenium based and/or bifunctional catalysts with metals might also be proper candidates for erythritol conversion to 1,3-butadiene.

The scope of the current work is to explore the single-step HDO of erythritol to 1,3-butadiene with the main objective of developing a series of heterogeneous transition metal oxide catalysts maximizing butadiene yield and productivity at shorter reaction time and lower catalyst to erythritol ratio so as to improve the viability of the envisaged process. A series of rhenium, molybdenum and mixed molybdenum-rhenium catalysts supported carbon black with different metal loadings, are synthesized and evaluated under specified reaction conditions. In addition to extensive testing under reaction conditions, the catalysts are characterized by employing basic (XRD, TPR and BET) and advanced (XPS and CH_3OH-TPSR) techniques. The novelty of the work lies in the use of mixed molybdenum-rhenium supported materials which are tested for the first time in the direct conversion of erythritol to 1,3-butadiene. This approach results in almost double butadiene productivity, achieved within a remarkably lower reaction time compared to the existing studies in open literature enhancing the efficiency of the process.

2. Materials and methods

2.1. Catalyst preparation

The catalytic materials were prepared by wet impregnation method using the commercially available carbon black (CB) Vulcan XC72. Molybdenum based catalysts (Mo/CB), tungsten based catalysts (W/CB) and rhenium based catalysts (Re/CB) were synthesized following the same procedure previously described [39] using ammonium molybdate as precursor ($(NH_4)_6Mo_7O_{24}{\cdot}4\ H_2O$) (Panreac), ammonium tungstate ($(NH_4)_{10}W_{12}O_{41}{\cdot}5H_2O$) (Sigma Aldrich) and ammonium perrhenate (NH_4ReO_4) (Thermo Fischer Scientific), respectively, while the calcination conditions were adjusted in order to avoid carbon burn off. More specifically, the calcination step was performed at 500 °C under inert flow (N_2) instead of oxidizing atmosphere (air flow) for 3 h. For mixed Mo-Re/CB catalysts, first the Mo/CB was impregnated using the same procedure as previously mentioned (drying and calcination) followed by impregnation of rhenium precursor. In an effort to determine the effect of calcination atmosphere, calcination of Mo-Re/CB was also conducted under air flow and at lower temperature (300 °C). For the catalysts calcined under oxidizing atmosphere an OXID subscript signifies the different calcination atmosphere. The nominal metal loading wt% and the calcination conditions of the catalytic materials are summarized in Table 1.

2.2. Catalyst characterization

The Brunauer-Emmet-Teller (BET) surface area and porosity of all fresh catalytic materials, as well as that of supports were determined by N_2 physisorption at 77.35 K using a Quantachrome Nova 2000e analyzer.

Thermogravimetric Analysis (TGA) experiments were carried out on a TG 209 F3 Tarsus, (NETZSCH, Germany) apparatus installed in the Laboratory of Petrochemical Technology (Chemical Engineering Department, AUTh). A small amount of the sample was placed in an alumina sample cup and heated up to 800 °C at a heating rate of 10 °C/min, under inert (N_2) atmosphere (50 cm^3/min).

The X-ray diffractometry (XRD) technique was employed in order to verify the crystallographic phases of fresh and used catalysts. The X-ray diffraction patterns of the samples were obtained by using a Bruker D8 Advance diffractometer, installed in Chemical Engineering Department (AUTh), with CuKa radiation ($\lambda = 0.15406$ nm) over $2\theta = 10°$ to 90°, at a scan rate of 0.5 s/point and step 0.02°.

The reducibility of the catalysts was tested via H_2 temperature programmed reduction (TPR). The experiments were performed in a gas flow system equipped with a quadrupole mass analyzer (OMNIStarTM, PFEIFFER, Germany). Typically, 0.15 g of catalyst was placed in a U – shaped quartz reactor and pretreated in a flowing He, for 0.5 h at 250 °C, followed by cooling to room temperature. After pretreatment, the temperature was raised from room temperature up to 800 °C at a rate of 10 °C/min in a 10 %H_2/He flow. The fragments of the following mass to charge ratios were recorded: 4(He), 2(H_2), 18(H_2O). All the measurements were performed in a flow unit located in the Laboratory of Petrochemical Technology (Chemical Engineering Department, AUTh). The unit is fully automated as all functions are controlled by the Genie Advantech software. There are two identical groups of gas inlet lines, each one consisting of four lines with an equivalent number of electronic flow controllers (Brooks Smart).

Temperature programmed surface reaction spectroscopy studies (TPSR) using methanol (CH_3OH-TPSR) were performed to study the nature of the catalyst active sites. The experiments were conducted in the above-mentioned homemade apparatus as previously described[38]. The following masses were recorded: 4(He), 15(CH_4), 18(H_2O), 29 (HCHO), 31(CH_3OH), 44(CO_2), 46(dimethyl ether, DME) and 60(methyl formate, $HCOOCH_3$) and the overlapping fragmentations of the compounds were appropriately considered.

Temperature programmed desorption experiments with helium (He-TPD) were carried out to used samples to identify the adsorbed species on the catalyst surface area. The experiments were performed in the above-mentioned homemade apparatus applying a two-step procedure. During the initial preheating step, the catalytic material was heated up to 100 °C for 0.5 h under He flow and then cooled down to room temperature. Then the sample was heated up to 800 °C with a heating rate of 10 °C/min. The following masses were recorded: 43(butane), 54(1,3-butadiene), 56(Butenes), 57(3-butene-1,2-diol) and 61(erythritol) and the overlapping fragmentations of the compounds were appropriately considered. The calculation of deposited 1,3-butadiene, butenes and butane on catalyst surface was performed based on calibration standards by using each gas compound separately and by tracking their *m/z* signals.

Temperature programmed desorption experiments with NH_3 (NH_3-TPD) were applied to study the acidic characteristics of the catalysts. Typically, 0.1 g of the sample was loaded in a fixed-bed quartz reactor and pretreated at 500 °C in He flow for one hour and then cooled down to 100 °C under He flow. Adsorption of ammonia was then performed with a flow of 5 % NH_3/He for 1 h at 100 °C. After flushing with pure He at 100 °C for 12 h to remove the physiosorbed ammonia, TPD analysis was carried out from 100 to 800 °C at a heating rate of 10 °C/min in helium. The composition of the exit gas was monitored on line with a quadrupole mass analysis (Omnistar, Balzer) located at the Chemical Process & Energy Resources Institute of the Center of Research and Technology Hellas (CPERI/CERTH). The following masses were recorded: 17, 16, 15 (NH_3), 18 (H_2O), 28 (N_2), 30 (NO), 44 (N_2O) and the overlapping fragmentations of the compounds were appropriately

Table 1
List of synthesized catalysts, **nominal** metal loading and calcination atmosphere.

Entry	Catalytic material	Metal1 (wt %)	Metal2 (wt %)	Calcination atmosphere
1	20Re/CB	20		Inert
2	5Re/CB	5		Inert
3	2Re/CB	2		Inert
4	20Mo/CB	20		Inert
5	5Mo−10Re/CB	5	10	Inert
6	10Mo−5Re/CB	10	5	Inert
7	5Mo−10Re/CB_{OXID}	5	10	Oxidizing
8	20 W/CB	20		Inert

considered.

XPS measurements were performed on a Kratos Analytical AXIS ultra DLD spectrometer equipped with and aluminum monochromatic X-ray source (λKα=1486.6 eV). The wide scan spectra were recorded by applying 7 mA/10 kV on X-ray source with pass energy of 160 eV. High resolution (HR) regions were recorded with pass energy of 20 eV on the analyzer during a three-sweep scan applying 10 mA/15 kV on X-ray gun. Binding energy referencing was employed based on C 1 s peak at 284.6±0.1 eV for the C-C bonds. Before XPS measurements the samples were stored under vacuum and the analysis was conducted on the same day.

2.3. Catalytic activity tests

Erythritol HDO activity tests were performed in liquid phase in an autoclave reactor operating in batch mode (80 ml) installed at the Institute of Catalysis Research and Technology (IKFT) at Karlsruhe Institute of Technology (KIT). A PTFE (polytetrafluoroethylene, teflon) liner was inserted in the reactor to reduce the volume at half. Typically, 0.5 g erythritol (Thermo Scientific) in 9.5 ml solvent (1,4-dioxane) (VWR Chemicals), along with 0.3 g (unless otherwise stated) catalyst were added in the reactor with a magnetic stirring bar. After sealing the autoclave, the air content was removed by flushing with argon. Afterwards, H_2 was added and adjusted to reach the desired pressure, while the autoclave was heated to reach the appropriate temperature under magnetic stirring. Both pressure and temperature inside the autoclave were monitored using a mechanical pressure gauge and a type K thermocouple respectively. The time at which the reactor reached the set point was considered at zero time. After a specific reaction time, heating and stirring were turned off and the reactor was forced to immediately cool down to room temperature. After having reached room temperature, the gas phase was collected in a gas sampling bag. In addition, the liquid phase along with the catalyst was diluted with distilled water (1:10) and remained under stirring for 2 minutes to completely dissolve the remaining solid erythritol. Then, the catalyst was separated from the liquid phase through vacuum filtration. The liquid products were quantified using a gas chromatograph (Agilent 7890B) equipped with a flame ionization detector and a capillary column (Stabilwax q/integra quard 30 m, 0.25 mm i.d 0.25 μm). Before analysis, liquid samples were diluted 10 times with tetrahydroxyfuran (THF) (VWR Chemicals). Gas products were analyzed in a gas Chromatography (Agilent 6890) equipped with both TCD and FID detector and two columns in series/bypass configuration (Hayesep Q 2 m, 2 mm i.d and Molsieve 5 A 80/100 2 m, 2 mm i.d). Carbon balance of all experiments was 96±2 %.

Typical reaction conditions for catalyst screening experiments were the following: 0.5 g erythritol, 4.5 ml 1,4-dioxane, 0.3 g catalyst, 140 °C reaction temperature, 60 bar initial H_2 pressure and 18 h reaction time. The reaction parameters were varied to study their effect and the details are described in each case. Another parameter that was explored was the effect of prereduction of the materials which was performed at specified temperature under 10 %H_2/N_2 for 1 h.

The descriptors that were used for the evaluation of the catalysts were the conversion of erythritol (Eq. (1)), the carbon-based products selectivity (based on the reactant consumed) (Eq. (2)) and carbon balance (Eq. (3)) were calculated as following:

$$\text{Erythritol conversion}(\%) = \frac{n_{feed,in} - n_{feed,fin}}{n_{feed,in}} \bullet 100 \quad (1)$$

$$\text{Selectivity}_{product,i}(\%) = \frac{n_{c,product,i}}{n_{c,feed,in} - n_{c,feed,fin}} \bullet 100 \quad (2)$$

$$\text{Carbon Balance}(\%) = \frac{\sum n_{c,product,i} + n_{c,feed,fin}}{n_{c,feed,in}} \bullet 100 \quad (3)$$

where $n_{feed,in}$ and $n_{feed,fin}$ are the initial and final moles of the feed, $n_{c,i}$ are carbon moles of the product i and $n_{c,feed,in}$ and $n_{c,feed,fin}$ are the initial and final carbon moles of the feed.

3. Results and discussion

3.1. Catalyst characterization

Table 2 summarizes the BET surface area of the fresh catalytic materials and their corresponding support. The BET surface areas of all materials are considerably lower than that of the support most probably due to pore blockage by the deposited oxide. As expected, the BET surface of 2Re/CB and 5Re/CB is close to that of the support due to the relatively low Re loading. The almost similar BET area for both 20Re/CB and 20Mo/CB catalysts can be attributed to their similar metal loading. The higher BET surface area of 20 W/CB compared to both 20Re/CB and 20Mo/CB can be attributed to the different crystal structures of the materials, which for 20 W/CB resembles a nanocrystalline one, as it is indicated from XRD results and will be explained later. In the case of mixed Mo-Re/CB catalysts, the surface is slightly higher compared to the one of both Mo- and Re/CB probably due to the small increase in the pore volume of the catalysts. However, the similarity in surface area implies that the catalyst structure is not affected by the impregnation of different loadings. It is also interesting to observe that for 5Mo-10Re/CB catalyst the calcination atmosphere slightly affects the BET surface area as the 5Mo-10Re/CB $_{OXID}$ presents a smaller BET surface compared to that of 5Mo-10Re/CB (147 and 187 m^2/g respectively) probably due to pore blocking of the nitrates which remained after calcination.

Fig. 1 depicts the TGA profiles of all catalytic materials under inert (N_2) atmosphere. Almost all the fresh materials are stable up to 700 °C, with an approximately 2 % weight loss which is attributed to the presence of various impurities that were not completely removed during calcination. However, from Fig. 1a it can be easily seen that the 20Re/CB fresh catalyst presents in total 8 wt% weight loss which starts at 350 °C and is extended until 700 °C. This implies that the intermediate rhenium species were not sufficiently removed during calcination as it was the case for the other fresh supported catalysts. Considering that in NH_4ReO_4 the weight loss (43 %) occurs in the same temperature range (Fig. 1a), it is concluded that a moderate percentage of the ammonium precursor salts were not removed during the calcination under N_2 flow. In addition, by comparing the various Mo-Re/CB catalysts (Fig. 1b), it seems that the calcination conditions have a slight impact on the materials, as the 5Mo-10Re/CB_{OXID} catalyst presents in total 4 wt% loss which starts at 400 °C. The latter indicates that the low calcination temperature applied under oxidizing atmosphere (300 °C) was not sufficient to completely decompose the NH_4ReO_4 species and/or ammonium molybdate. TGA profile of ammonium molybdate (Fig. 1b) indicates that a total weight loss of 17 % occurs until 300 °C, while after it remains stable. This suggests that the corresponding weight loss of 5Mo-10Re/CB_{OXID} is ascribed to NH_4ReO_4 species that were not removed as their weight loss appears at the same range with that of 5Mo-10Re/CB_{OXID}. It was found that the 60 % of NH_4ReO_4 was removed after calcination at low temperature.

XRD analysis was carried out to investigate the structure of each material and the diffractograms are presented in Fig. 2. In a few cases of

Table 2
BET surface areas of fresh catalytic materials and supports.

Material	BET surface area (m^2/g)	Pore volume (cm^3/g)
Carbon Black CB	250	1.20
20Re/CB	150	0.40
2Re/CB	274	1.30
5Re/CB	219	1.40
20Mo/CB	149	0.38
5Mo−10Re/CB	187	0.48
10Mo−5Re/CB	182	0.49
5Mo−10Re/CB_{OXID}	147	1.20
20 W/CB	208	0.54

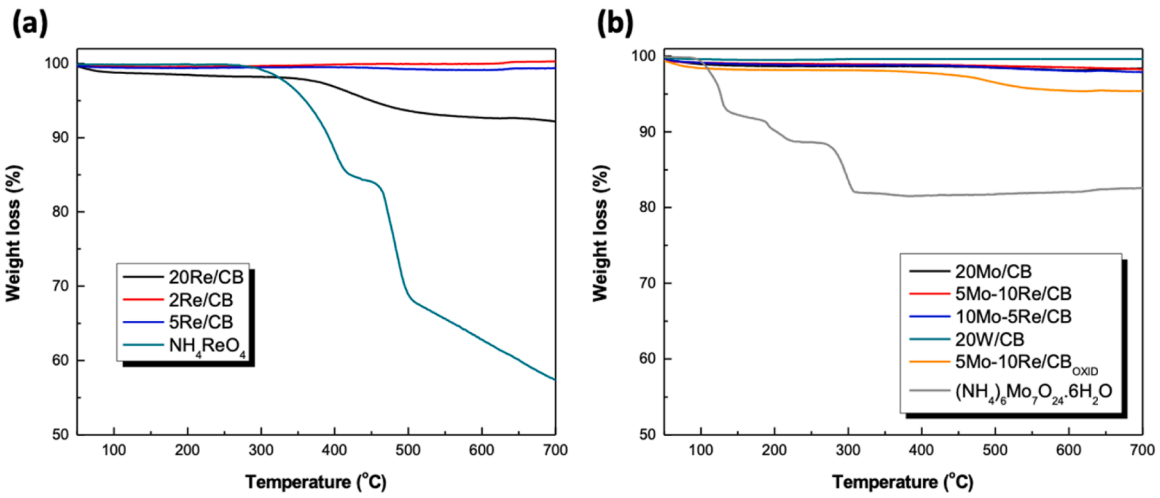

Fig. 1. TGA profiles of fresh catalytic materials and their precursors under inert (N_2) atmosphere.

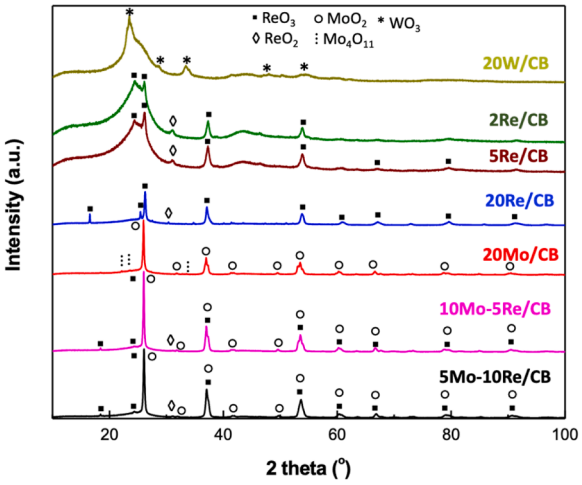

Fig. 2. XRD graphs of fresh catalytic materials.

CB-based catalysts it is interesting to observe the formation of low intensity peaks of reduced oxides along with their oxidized forms. This difference can be attributed to different calcination conditions applied. The presence of carbon black as support in combination with N_2 atmosphere during calcination at high temperature (500 °C) may enhance the reducibility of the deposited oxides. The XRD graphs of the samples with various Re loadings revealed that Re crystallizes mostly as ReO_3. A slight shift of the diffraction peaks to higher 2θ in the samples was observed compared to the reference pattern (JCPDS: 00–24–1009) indicating an intra-layer shrinkage and thus a decrease in lattice constant[40]. The diffraction pattern of the sample with the high loading (20 wt%) displays more distinct ReO_3 peaks compared to the samples with 2 and 5 wt % in which the peaks are broad. As expected, an increase in crystallite size of the materials is observed with increasing metal loading. More specifically, the crystallite size of the catalyst with 2 and 5 wt% is quite close and different with that of 20Re/CB (2Re/CB: 13.6 nm, 5Re/CB: 15.2 nm, 20Re/CB: 21.1 nm). XRD graph of 20Mo/CB catalyst, show diffraction peaks of MoO_2 (JCPDS: 65–5787), whereas a few low intensity peaks of Mo_4O_{11} are also observed. On the other hand, both spectra of Mo-Re/CB catalysts resemble that of 20Re/CB as well as of 20Mo/CB catalyst. It is difficult to distinguish between ReO_3 and MoO_2, as their peaks appear at almost similar 2θ values. Therefore, it can be assumed that Mo-Re/CB samples contain both ReO_3 and MoO_2, although it is not possible to assign each peak to a specific phase. It is interesting to note that impregnation of Mo on Re-based materials resulted also in a decrease in crystallite size of the materials (5Mo-10Re/CB: 14.4 nm, 10Mo-5Re/CB: 14.6 nm) compared Re/CB materials with metal loading higher than 5 wt%, implying a better a dispersion of the metals due to their coexistence on the catalyst surface. This is consistent with the shift of reduction temperature observed in H_2-TPR graphs mentioned below. Lastly, the XRD spectrum of the 20 W/CB catalyst shows that WO_3 (JCPDS: 43–1035) is the main crystal phase detected at very low intensities with wide peaks indicative of low crystallinity of the fresh catalytic material.

The reducibility of supported catalytic materials was investigated via temperature programmed reduction (H_2-TPR) and their profiles are presented in Fig. 3. All the Re-based materials irrespective of their loading, show two reduction peaks centered at 300 and 420 °C indicating the presence of different rhenium oxide species. In the open literature there is no clear consensus regarding the reduction temperature of rhenium. Therefore, it can be assumed that during H_2-TPR experiment the high valent Re species were partially reduced to Re^{4+}, while the formation of metallic Re cannot be completely excluded. Quantification of the total H_2-consumption during H_2-TPR experiments showed that for 20Re/CB, after reduction part of rhenium may be present with valence lower than + 4 considering that the initial valence is 6 + according to XRD mentioned in the previous paragraph. For the other two samples (2 and 5 wt% Re) the quantification of H_2 profiles also revealed that at temperatures over 500 °C rhenium suboxides with

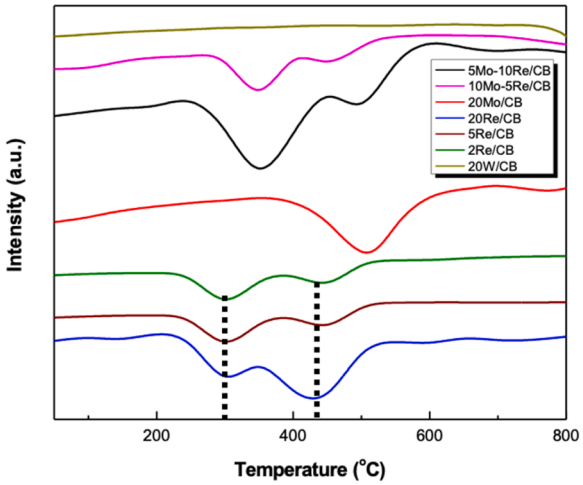

Fig. 3. H_2-TPR results of fresh catalytic materials.

valence lower than 4 + are formed. The reduction peak of the 20Mo/CB catalyst is centered at 500 °C, which is considerably higher to that of 20Re/CB owing to the harder reducibility of molybdenum species compared to rhenium[41]. The peak is assigned to the reduction of MoO_3 to MoO_2[39], while the calculated consumption of H_2 corresponds to ~25 % of the theoretical one for the reduction of Mo^{6+} to Mo^{4+}. Even though the MoO_3 phase was not detected in the XRD graphs it could be suggested that the fully oxidized species are amorphous and/or highly dispersed. The presence of Mo^{6+} species on the catalyst surface was also confirmed by the XPS measurements as will be explained in Section 3.2.8 (effect of synthesis parameters). In the case of both Mo-Re/CB catalysts two reduction peaks are observed at 350 °C and 470–500 °C. The first peak can be ascribed to rhenium reduction which has shifted to higher temperatures compared to Re-based materials. Considering the presence of different rhenium oxides along with molybdenum ones, a closer look at Fig. 3 (for 5Mo-10Re/CB) reveals that the second peak appears at almost the same temperature, 470 °C instead of 500 °C, with that of Mo/CB. This moderate shift of molybdenum reduction peaks, at temperatures lower than 500 °C, has been previously reported by Herrera et al.,[41] as Re facilitates the reduction of molybdenum oxides implying a strong interaction between molybdenum and rhenium as well (in accordance with XRD results). The differences in the reduction temperature of both Re and Mo oxides implies an interaction of metals which may modify or create new sites[42].

3.2. Catalyst performance evaluation

3.2.1. Catalyst screening

The performance of the catalytic materials with 20 wt% loading, as well as that of both Mo-Re/CB, in erythritol hydrodeoxygenation evaluated at 140 °C and under 60 bar initial H_2 for 18 h, is summarized in Table 3 for the fresh materials and in Table 4 for the reduced ones. The latter were prereduced under H_2 flow under 1 h in a specified temperature for each material mentioned in Table 4. This temperature was based on the H_2-TPR results presented in Fig. 3. It is known that both homogeneous and heterogenous rhenium-based catalysts are very active catalysts for erythritol HDO[31–33]. The results from both tables confirm that indeed rhenium-based materials are promising catalysts for erythritol HDO, as they exhibit higher activity, in comparison with 20Mo/CB and 20 W/CB which present very low activity towards converting erythritol. However, production of 1,3-butadiene was not observed at all in any case, contrary to butenes and/or butane, the formation of which was highly promoted, implying that the extended reaction time applied (18 h) most likely promotes its further conversion towards butenes/butane.

Among the fresh catalysts tested (Table 3), even though the 20Re/CB reached the highest conversion level (57 %), the production of partially deoxygenated products such as butenediol and butanediols, is also observed with a total of 6.7 % selectivity in addition to butane which was the main product detected. Over fresh 20Mo/CB, regardless of the low conversion level (14 %), butenes are the main products detected in gas phase (entry 2) with 99 % selectivity. The fact that butane production is not observed despite the extended reaction times is assigned to the mild hydrogenation activity of molybdenum catalysts which do not promote the hydrogenation of C=C[38,39], especially at the low reaction temperatures used. On the other hand, both mixed Mo-Re/CB catalysts demonstrate promising performance with a similar product spectrum (entries 3 and 4), while the production of butanediols is eliminated compared to 20Re/CB. Another common feature over Mo-Re/CB catalysts is the presence of butenes and butane, implying that the complete hydrogenation of the former to the latter is not completely favored even after 18 h. This might be ascribed to the presence of molybdenum, demonstrating that the impregnation of rhenium-based catalysts with other metals is necessary to avoid C=C rupture, in agreement with the work of Yamaguchi et al.[33]. Mild hydrogenation activity of Mo can be further confirmed by comparing the catalytic activity of 20Re/CB (entry 1) with 5Mo-10Re/CB (entry 3), as both attained iso-conversion levels. Butane production is highly promoted over 20Re/CB, while butenes are formed at low selectivity values. In contrast, impregnation of Mo over Re/CB enhanced butenes selectivity by simultaneously restricting butane production. In both cases the sum of selectivity values of butenes and butane is similar confirming the importance of adding Mo on Re-based materials to avoid the C=C bond rupture of butadiene. Lastly, over the 20 W/CB catalyst, erythritol conversion does not exceed 11 % (entry 5), while the production of products with less than 4 carbon atoms (such as CH_4, C_2H_6), is promoted, indicating that tungsten enhances C-C bond cleavage.

All the above catalytic materials, except for 20 W/CB, were also applied in erythritol HDO after reduction. The reduced 20 W/CB catalyst was not studied due to reaction temperature limitation, as it requires extremely high temperatures (Fig. 3) to reduce it.

It is interesting to observe that conversion levels over reduced materials (Table 6) are noticeably lower in most of the cases compared to the non-reduced ones implying that the coexistence of both oxidized and reduced species (as it is indicated from the XRD of the non-reduced samples) boosts erythritol conversion. Among the reduced catalysts (Table 4), all rhenium-based catalysts display a satisfactory activity for erythritol conversion, while the production of the intermediate products is restricted mostly in the case of Mo-Re/CB catalysts (entries 3 and 4) underlying once again the benefit of using molybdenum as a modifier. Another important feature of the reduced samples is that the production of gaseous products with less than 4 carbon atoms is slightly higher implying that the reduced species along with the extended reaction times promote C-C bond scission.

The above results clearly point to the promising performance of rhenium and mixed rhenium-based catalysts in erythritol HDO. However, due to the extended reaction time applied, most of them showed high selectivities to hydrogenated C_4 products which are possibly formed from 1,3-butadiene via sequential hydrogenations (Scheme 1). The activity of 20Re/CB and both Mo-Re/CB catalysts, as they exhibited the best performance in terms of conversion and product distribution, was further evaluated at a substantially shorter reaction time of 5 h. In addition, to study also the effect of rhenium loading, two more catalysts with 2 and 5 wt% loading were tested. Apart from the reaction duration, all the other operating variables were kept the same. The results obtained are tabulated in Table 5. The activity of the Re/CB catalysts (entries 1–3) seems to be directly related to Re as it increases linearly with its loading. It is clear that shorter reaction times indeed favor 1,3-

Table 3
Erythritol conversion and product distribution over fresh unreduced metal oxides (T = 140 °C, $P_{in,H2}$ = 60 bar, catalyst/substrate ratio = 0.56 $g_{cat}/g_{erythritol}$ and t = 18 h).

			Product selectivities (Carbon based %)					
Entry	Catalyst	Conversion (%)	Butenes	Butane	3-Butene−1,2-diol	Butanediols	Butanols	Others*
1	20Re/CB	57	11	81	0.3	7	3	2
2	20Mo/CB	14	99	-	2	1	-	-
3	5Mo−10Re/CB	56	29	63	-	3	2	1
4	10Mo−5Re/CB	48	21	79	-	1	-	1
5	20 W/CB	10	3	65	14	15	-	6

* Others: CO_2 – CH_4 – C_2H_6 – C_3H_8.

Table 4
Erythritol conversion and product distribution over reduced metal oxides. (T = 140 °C, $P_{in,H2}$ = 60 bar, catalyst/substrate ratio = 0.56 $g_{cat}/g_{erythritol}$ and t = 18 h).

			Product selectivities (%)					
Entry	Catalyst (Reduction Temperature,°C)	Conversion (%)	Butenes	Butane	3-Butene−1,2-diol	Butanediols	Butanols	Others*
1	20Re/CB (400)	36	10	33	-	57	1	4
2	20Mo/CB (500)	18	58	-	10	26	4	5
3	5Mo−10Re/CB (400)	33	6	87	-	-	-	8
4	10Mo−5Re/CB (400)	29	10	79	-	8	4	9

* Others: CO_2 – CH_4 – C_2H_6 – C_3H_8.

Table 5
Erythritol conversion and product distribution over rhenium and mixed rhenium-based catalysts. (T = 140 °C, $P_{in,H2}$ = 60 bar, catalyst/substrate ratio = 0.56 $g_{cat}/g_{erythritol}$ and t = 5 h).

			Product selectivities (%)						Productivity
Entry	Catalyst	Conversion (%)	1,3-Butadiene	Butenes	Butane	3-Butene−1,2-diol	Butanediols	Butanols	(g_{BD}/g_{cat}h)
1	2Re/CB	8	-	39	-	57	1	-	-
2	5Re/CB	18	-	69	-	26	5	-	-
3	20Re/CB	65	88	5	-	3	0.7	-	0.091
4	5Mo−10Re/CB	51	93	4	-	4	0.2	-	0.075
5	10Mo−5Re/CB	39	92	2	-	6	-	3	0.051

*Others: CO_2 – CH_4 – C_2H_6 – C_3H_8.

butadiene as it is produced in most of the cases, along with other C_4 products. The main product obtained over 2Re/CB (entry 1) is 3-butene-1,2-diol followed by butenes, while the conversion level is relatively low (< 10 %), probably due to the low Re loading. The same product distribution, with butenes being the most dominant species instead of 3-butene-1,2-diol, is also observed over 5Re/CB with the conversion now reaching almost 20 % (entry 2). Compared with entry 3, it is interesting to observe that over the rhenium-enriched catalyst (20Re/CB), not only 1,3-butadiene is the major product formed (88 % selectivity), but the highest conversion level equal to 65 % is achieved. The differences in the selectivity can be attributed to the variation of the H_2/erythritol ratio obtained in every case. Generally, the initial H_2/erythritol molar ratio in each run equals to 24, however in the presence of 2Re/CB and 5Re/CB due to the relatively low conversion of erythritol, the above ratio (based on consumed erythritol) drastically changes increasing to 270 and 127, respectively, while for 20Re/CB the change in the ratio is moderate, 35. Thus, this excess of hydrogen in the closed batch system most likely promotes butenes production via 1,3-butadiene hydrogenation. Another important fact that can explain these differences might be the different rhenium loadings which affects the catalyst structure as it was demonstrated from XRD results mentioned above. More specifically, impregnation of different Re loadings affects the crystallite size of the materials, as it is already mentioned above in the XRD results, which is lower for both 2Re/CB and 5Re/CB in comparison with 20Re/CB. The smaller crystallites may induce changes in product selectivity (structure sensitivity) in addition to those ascribed to the differences in H_2 availability mentioned above. However, in order to avoid using high rhenium loadings on accounts of high metal cost[43], the addition of molybdenum is studied in catalysts with lower rhenium amount. From entries 4 and 5, it can be easily observed that 1,3-butadiene selectivity is greatly modified by adding molybdenum, while conversion attains a satisfactory level of approximately 40 and 50 % for 10Mo-5Re/CB and 5Mo-10Re/CB, respectively. Not only the production of the intermediate products is eliminated by impregnating molybdenum, but the catalysts containing Mo and Re maintain the C=C of 1, 3-butadiene as well, owing to their mild hydrogenation activity [38, 39]. The productivity of butadiene production (Table 5) was also calculated to further evaluate the current results. Although over 20Re/CB the highest productivity value is achieved (0.091 g_{BD}/g_{cat}h), promising and quite comparable values are also obtained in the presence of 5Mo-10Re/CB (0.075 g_{BD}/g_{cat}h) demonstrating the promising performance of mixed Mo-Re based catalysts towards converting erythritol to butadiene. For Re based materials with low metal loadings (2–5 wt%), as no butadiene was formed, its productivity is zero. As both Mo-Re/CB catalysts present promising activity, they were chosen as catalysts to study the evolution of erythritol HDO conversion with time on stream (TOS).

The temperature programmed surface reaction spectrometry technique using methanol (CH_3OH-TPSR) as probe molecule was applied to gain information about the nature of the available species on the catalytic surface. CH_3OH-TPSR is a very well-known technique which has attracted a lot the scientific interest mostly towards identifying the nature of the species (redox, acid, basic) on catalytic surface, as well as elucidating the reaction mechanism[38,44–47]. Methanol is considered the most suitable molecule as during its oxidation the product distribution provides fundamental information about the nature of the existing species on the surface. More specifically, it is known that redox species convert methanol to formaldehyde, acid sites lead to dimethyl ether (DME) and methyl formate ($HCOOCH_3$), while CO_2 is formed in the presence of basic species[38,47]. CH_3OH-TPSR experiments were performed for 5Re/CB and 5Mo-10Re/CB as over these materials the product distribution varies significantly, and their profiles are presented in Fig. 4. The main common feature of all spectra is methanol's desorption peak which appears at high temperatures (> 300 °C). As it is well known that the desorption of molecularly physisorbed methanol occurs at low temperatures (100 °C), its desorption peak at higher temperatures is attributed to the self-hydrogenation of surface methoxy species (*OCH_3) and hydroxyl groups which desorb as CH_3OH through protonation [45,48,49]. This mostly comes together with DME and HCHO formation, as it is the case in all profiles, especially when the concentration of these species is abundant [38]. In most of the cases the products formed desorb at more than one temperature zone implying the presence of methoxy species adsorbed at different sites[45]. Another common aspect is CH_4 production which originates either from decomposition of both CH_3OH and DME and/or their hydrogenolysis [50]. As it has been previously mentioned [38], the peak at low temperature corresponds to hydrogenolysis, while that at high temperature to decomposition [50]. Water desorption peaks are also detected, as it is released through methanol reactions associated with DME and methyl formate, however, these peaks are not included in the figures for simplicity.

By comparing the CH_3OH-TPSR spectrum of 5Re/CB (Fig. 4a) and

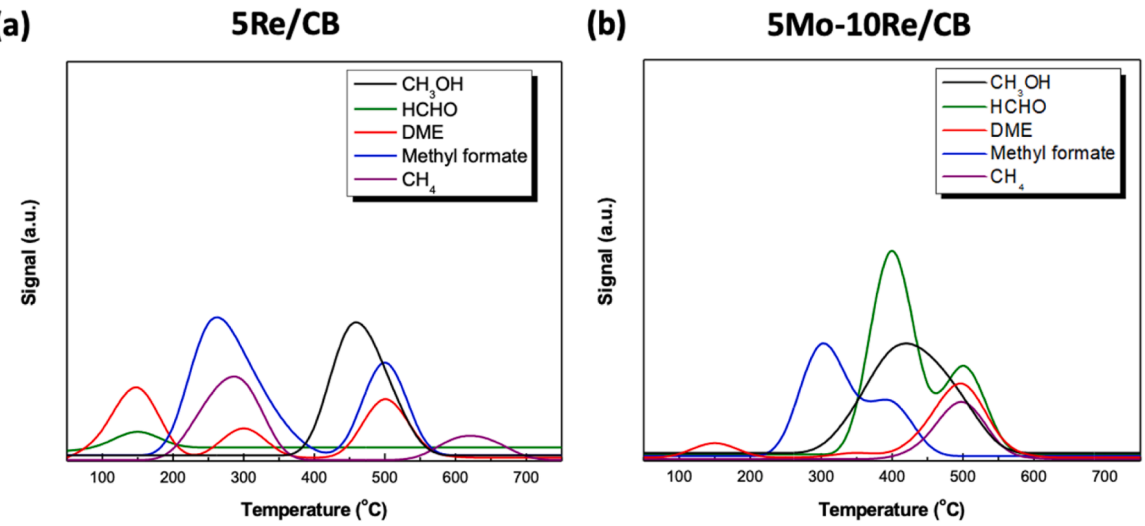

Fig. 4. CH_3OH-TPSR spectrum of fresh (a) 5 %Re/CB and (b) 5 %Mo-10 %Re/CB. (The following masses were used: $m/z = 31$ for CH_3OH, $m/z = 30$ for HCHO, $m/z = 44$ for CO_2, $m/z = 45$ for DME, $m/z = 60$ for $HCOOCH_3$ and $m/z = 15$ for CH_4).

5Mo-10Re/CB (Fig. 4b), the same desorption products are observed, such as HCHO, DME and methyl formate, nonetheless at different temperature zones and intensities (concentrations). Despite the absence of any quantification, it can be concluded that both materials host redox and acid species. A closer look at the figures reveals that the intensity of the DME and methyl formate peaks are lower, however at the same order, over 5Mo-10Re/CB indicating the presence of active sites with different strength. Regarding redox species, only a small HCHO peak appears at 150 °C for 5Re/CB implying that this catalyst possesses a low amount of surface redox sites which are active at low temperature. In contrast, the incorporation of molybdenum has a strong impact on redox sites as HCHO production is greatly promoted. Two desorption peaks at 400 and 500 °C are observed with their intensity being one order of magnitude higher compared to that of 5Re/CB. In our previous study [38] it was found that the fresh Mo/CB catalyst contains both acid and redox species on the surface with their ratio being equal to 1. Both Mo/CB and 5Mo-10Re/CB catalysts maintain the same redox to acid ratio which is higher compared to 5Re/CB implying that impregnation of Mo on Re-based materials increases the amount of redox species on the catalytic surface (redox to acid ratio: Mo/CB: 1, 5Mo-10Re/CB: 1, 5Re/CB: 0.19). Considering that the removal of oxygen from erythritol proceeds via successive dehydration/hydrogenation steps the presence of both, acidic and redox sites, is essential for the formation of the C_4 products. Despite the very low intensity of the redox sites (HCHO) which can be translated to low population on the surface, the high selectivity to butenes instead of butadiene over Re/CB (Table 4) can be ascribed to the high hydrogenation activity of these sites as they appear in the low temperature regime of the desorption profile (Fig. 4a). In contrast, the high population of the redox sites on the surface of the 5Mo-10Re/CB which however appear in the high temperature region (400–500 °C) are not highly active in hydrogenation at the low reaction temperature used (140 °C). According to the experimental results presented in Table 5 entry 4, over the 5Mo-10Re/CB the butadiene selectivity remains high most likely because of the limited hydrogenation activity of the active redox sites. As both, the activity and the selectivity, were found to increase upon incorporation of molybdenum, it can be suggested that both, molybdenum and rhenium oxide species, act as redox as well as acid sites and are the most active ones during erythritol HDO towards 1,3-butadiene production. The acidity of those materials was measured by NH_3-TPD. Impregnation of Mo enhanced the acidity of the catalyst (5Re/CB: 0.21 $\mu mol_{NH3}/m^2_{BET}$, 5Mo-10Re/CB: 1.06 $\mu mol_{NH3}/m^2_{BET}$). The NH_3-TPD profiles of both 5Re/CB and 5Mo-10Re/CB (Fig. 5) show one desorption peak centered at relatively low

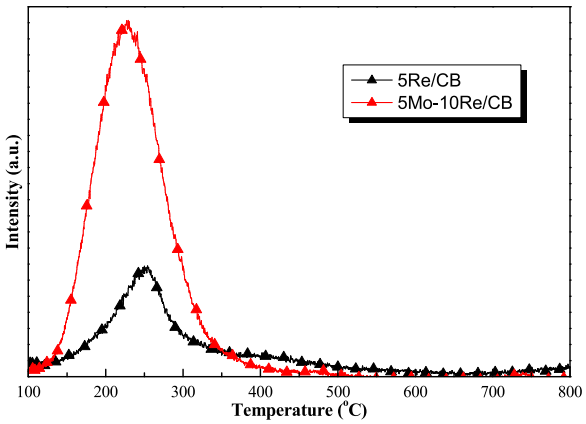

Fig. 5. NH_3-TPD profile of 5Re/CB and 5Mo-10Re/CB catalysts.

temperature (220–250 °C) demonstrating the presence of weak acid sites. For the 5Re/CB the peak centers to 250 °C, slightly higher temperature indicating an increase in the acid strength[51]. Additionally, a closer look in the graph, reveals for 5Re/CB catalyst, a not well resolved peak (between 350 – 500 °C) which is characteristic of acid sites with medium to high strength. This is consistent with the CH_3OH-TPSR results presented above which show the presence of the same acid species on the surface of both catalysts, nonetheless with different properties. In general, acidity is a key factor for enhanced HDO activity. However, acidity itself is not sufficient to explain the different catalytic activity, as the redox sites play also a crucial role in HDO reactions. It has been reported that the metal sites of a catalyst are responsible for promoting hydrogenation of olefinic compounds[51]. The CH_3OH-TPSR results indicated that although the population of redox species present on the surface of 5Re/CB is lower, they are more active compared to 5Mo-10Re/CB, as the product of methanol oxidation (HCHO) desorbed at low temperatures close to that of the HDO experiments. Therefore, it can be suggested that the low activity of 5Re/CB is attributed to its low acidity, while the presence of highly active redox sites favors butenes production indicative of high hydrogenation activity.

3.2.2. *Effect of reaction time over molybdenum-rhenium-based catalysts*

Erythritol conversion and product distribution over Mo-Re/CB catalysts monitored as function of reaction time is presented in Fig. 6. The same product trend is observed over the two Mo-Re/CB catalysts. 3-

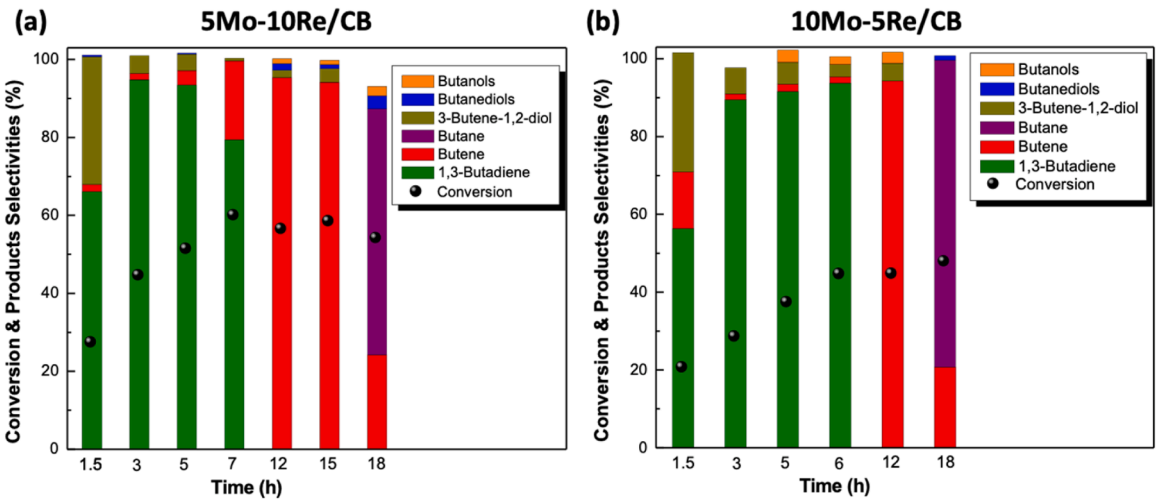

Fig. 6. Evolution of erythritol conversion over a) 5Mo-10Re/CB and b) 10Mo-5Re/CB. (T = 140 °C, $P_{in,H2}$ = 60 bar and catalyst/substrate ratio = 0.56 $g_{cat}/g_{erythritol}$).

Butene-1,2-diol, the first HDO product, is produced at short reaction times, while with progressive reaction time, its production becomes limited in favor of 1,3-butadiene, confirming that indeed the former is the precursor of the latter. Increasing the reaction time from 5 to 7 h the hydrogenation of 1,3-butadiene is promoted first in favor of butenes and then of butane. Over the 5Mo-10Re/CB catalyst the highest selectivity to 1,3-butadiene (93 %) is achieved at 5 h for 51 % erythritol conversion (Fig. 6a), while in the presence of 10Mo-5Re/CB the highest selectivity is 93 % at 6 h for 45 % conversion (Fig. 6b). As expected, conversion increases with reaction time up to a limit but more importantly, reaction time affects the product distribution. Long reaction times (> 7 h), have a negative impact on 1,3-butadiene selectivity by promoting firstly butenes and sequentially n-butane production. According to Scheme 1 the former is produced via hydrogenation of 1,3-butadiene and the latter via hydrogenation of butenes due to the combination of extended reaction times along with the presence of hydrogen.

In the presence of 5Mo-10Re/CB, it is important to notice that after 5 h, conversion slightly increases from 51 % to ~60 % and remains almost stable until 18 h. Leaching is a very common obstacle of rhenium-based catalysts applied in liquid reactions[52]. 'However, ICP analysis of the liquid phase after 18 h of reaction time did not detect any rhenium confirming that leaching should be excluded. This implies that catalyst deactivation possibly by adsorbed intermediates and/or products is the reason for the unchanged conversion with reaction time. Comparing Fig. 5a and b, even though the same product distribution is observed, the 5Mo-10Re/CB catalyst is approximately 30 % more active in terms of conversion compared to 10Mo-5Re/CB. As the XRD patterns of both materials (Fig. 2) show that the structure of the Mo-Re/CB catalysts remained the same by impregnating different loadings and the surface area of the catalysts is also similar, the results indicate that the presence of rhenium loadings between 5 % and 10 % along with molybdenum enhances the HDO ability of the catalyst. Based on activity, the 5Mo-10Re/CB was chosen as the most promising catalyst and was further used to study the effect of other reaction parameters.

3.2.3. *Effect of reaction temperature*

The product distribution for erythritol HDO at different reaction temperatures for 5 h reaction time is depicted in Fig. 7. As it was expected, elevating the temperature from 100 to 160 °C, erythritol conversion appreciably increases from 13 % to 58 %. The production of 3-butene-1,2-diol is mostly promoted at 100 °C, implying that low reaction temperatures do not fully promote HDO towards 1,3-butadiene. The gradual temperature increment to 140 °C, highly favors 1,3-butadiene production, as it is the main product observed achieving a maximum

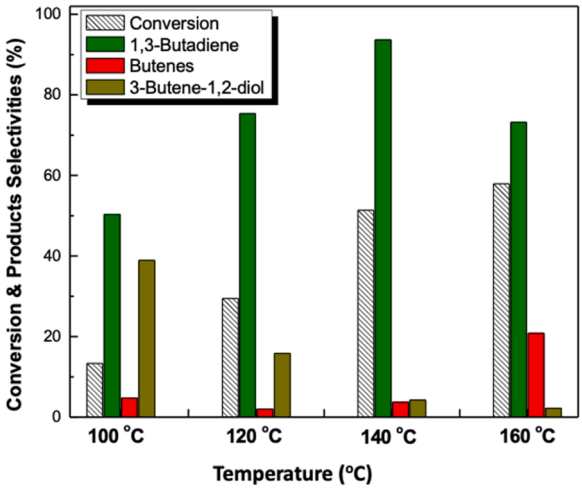

Fig. 7. Effect of reaction temperature on erythritol conversion and product distribution over 5Mo-10Re/CB. ($P_{in,H2}$ = 60 bar, catalyst/substrate ratio = 0.56 $g_{cat}/g_{erythritol}$ and t = 5 h).

selectivity value equal to 94 %. Further temperature increment to 160 °C, decreases its selectivity to 73 % with a subsequent formation of butenes (21 % selectivity), while erythritol conversion does not considerably change. Considering the above, 140 °C was chosen as the optimum reaction temperature for erythritol HDO to 1,3-butadiene over the 5Mo-10Re/CB catalyst.

The effect of reaction temperature on reaction rate was used to determine the apparent activation energy of erythritol HDO. Based on the Arrhenius plot depicted in Fig. 8, it is calculated that the apparent activation energy for erythritol HDO over 5Mo-10Re/CB is equal to 34 kJ/mol. However, the absent of studies in the open literature regarding the activation energy of erythritol makes it difficult to compare the current results. To the best of our knowledge, there is only one very recent work by Virgilio et al.[53], who reported activation energies of erythritol over $Ir/ReO_x/TiO_2$ at a higher temperature range (150–225 °C). They found that the overall erythritol consumption has an activation energy of 55.4 kJ/mol. Direct comparison of the two values is not possible due to the differences in the catalyst composition. It should be mentioned though that Virgilio et al. [53] calculated also the activation energies of the various routes of erythritol conversion and found that dehydration is the step with the highest activation energy

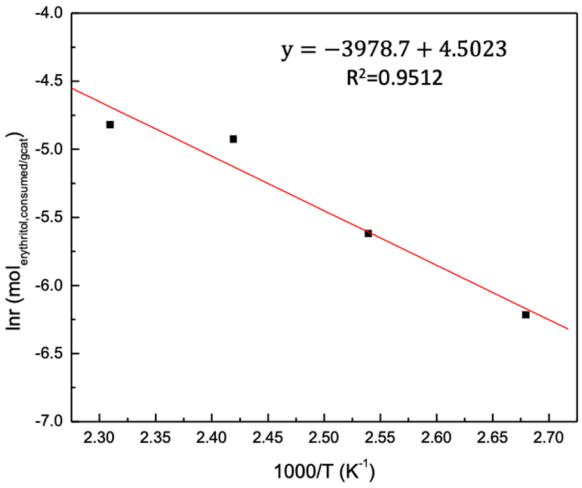

Fig. 8. Arrhenius plot for the overall reaction of erythritol HDO.

(212.21 kJ/mol) while isomerization exhibits the lowest (20 kJ/mol). They also found that the required activation energy for C-C bond hydrogenolysis is higher than the one for C-O bond (132.6 and 79.2 kJ/mol, respectively). The differences in activation energies interpret the observed product distribution. In the temperature range studied (100–160 °C), the formation of products derived through C-O bond hydrogenolysis scission is favored compared to C-C rupture. Products with lower that C4carbon atoms were not detected.

3.2.4. *Effect of H_2 pressure*

The effect of hydrogen pressure on erythritol HDO was investigated by carrying out the reaction at 20, 40 and 60 bar H_2 pressure, as well as at inert high pressure (60 bar Ar) at constant reaction temperature (140 °C), catalyst weight (catalyst/substrate ratio = 0.56 $g_{cat}/g_{erythritol}$) and reaction time (5 h). The results presented in Fig. 9 show that the effect of H_2 pressure is more significant on erythritol conversion compared to 1,3-butadiene production. Even at low pressures 1,3-butadiene selectivity reaches a high value of 83 % at 20 bar and it is increased up to almost 94 % at 60 bar. With increasing pressure, conversion increased from 34 % to 51 %, which can be attributed to a positive effect of hydrogen on the kinetics of erythritol consumption. On the other hand, under inert pressure erythritol did not react at all, emphasizing the utmost importance of hydrogen in the system.

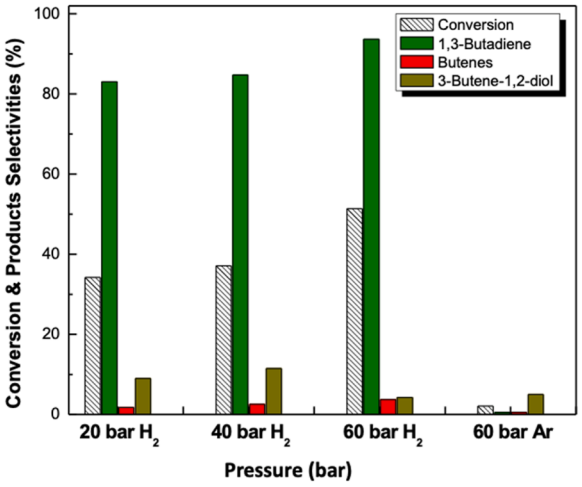

Fig. 9. Effect of hydrogen pressure on erythritol conversion and product distribution over 5Mo-10Re/CB. (T = 140 °C, catalyst/substrate ratio = 0.56 $g_{cat}/g_{erythritol}$ and t = 5 h).

3.2.5. *Effect of catalyst loading*

The effect of catalyst loading on erythritol conversion and product distribution was studied in the range of catalyst/substrate ratios from 0.19 to 1.18 $g_{cat}/g_{erythritol}$, while keeping the reaction temperature (140 °C), hydrogen pressure (60 bar) and reaction time (5 h) constant. As it was expected, erythritol conversion increases with catalyst loading (Fig. 10). However, it can be observed that erythritol conversion does not increase proportionally with catalyst loading implying possible mass transfer phenomena. At low catalyst loading, even though the conversion is low (15 %), butenes are produced instead of 1,3-butadiene. Butenes formation at low ratios is ascribed to the difference obtained in H_2/erythritol (based on consumed erythritol) as it was mentioned in Section 3.2.1 (H_2/erythritol = 162 for catalyst/substrate = 0.16 $g_{cat}/g_{erythritol}$, H_2/erythritol = 44 for catalyst/substrate = 0.56 $g_{cat}/g_{erythritol}$, H_2/erythritol = 40 for catalyst/substrate = 1.18 $g_{cat}/g_{erythritol}$). An increase of the catalyst amount to 0.56 $g_{cat}/g_{erythritol}$ leads to the highest 1,3-butadiene selectivity mainly owing to a higher conversion level compared to 0.19 $g_{cat}/g_{erythritol}$. In contrast, further increase up to 1.18 $g_{cat}/g_{erythritol}$, does not considerably affect the conversion, which increases from 51 % to 60 %. This is not followed by an increase in 1,3-butadiene selectivity but instead, by a loss due to its hydrogenation to butenes. It should be noted that in spite of the quite similar conversion level, the sum of 1,3-butadiene and butenes selectivity remains constant at both ratios. As the obtained H_2/erythritol molar ratio is approximately the same, it is suggested that butenes production is attributed to the increase of the catalyst active sites.

3.2.6. *Catalyst reusability*

Catalyst recovery and reusability is one of the most challenging aspects in heterogeneous catalysis from both economic and environmental point of view, especially for a commercial application [54]. Before catalyst reuse, the adsorbed species on the catalyst surface were determined by thermogravimetric analysis. Fig. 11 illustrates the variation in catalyst weight as a function of temperature under inert conditions. As it was previously mentioned, the profile of the fresh 5Mo-10Re/CB catalyst is almost flat. On the other hand, the used catalyst after 5 h, presents a total weight loss of 8 % which is extended from 150 to 400 °C. This weight loss can be attributed to water removal and/or to the remaining adsorbed organic species on the catalyst surface after the experiment. Therefore, the regeneration of the used 5Mo-10Re/CB after 5 h of testing was performed under N_2 flow at 400 °C for 1 h, as according to TGA results the removal of the adsorbed organic species from the catalyst surface occurs at this temperature. The TGA profile of the regenerated catalyst follows the same trend as that of the fresh one indicating that the desorbed species were sufficiently removed after N_2 treatment.

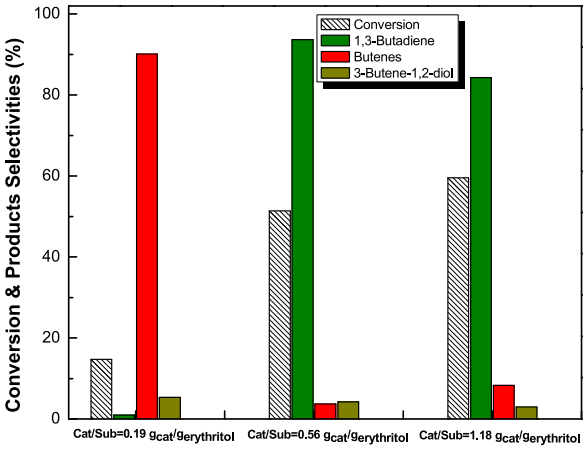

Fig. 10. Effect of catalyst/erythritol ratio (weight) on erythritol conversion and product distribution over 5Mo-10Re/CB. (T = 140 °C, $P_{in,H2}$ = 60 bar and t = 5 h).

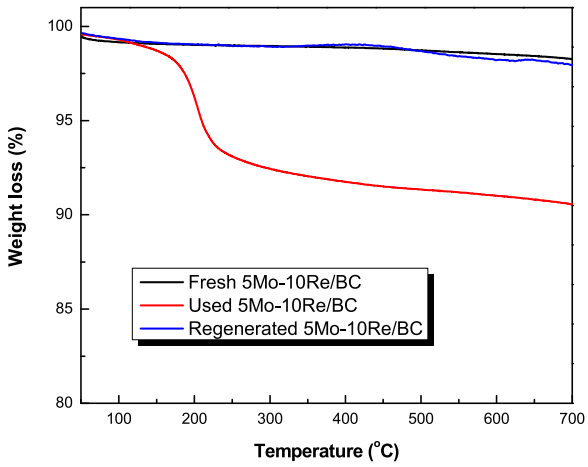

Fig. 11. TGA analysis of fresh (black line), used (red line) and regenerated (blue line) 5Mo-10Re/CB under inert (N_2) flow.

Temperature programmed desorption experiments with He (TPD-He) were performed with used samples to identify the adsorbed compounds on the catalyst surface. The He-TPD profile of the used catalyst is depicted in Fig. 12. As it was expected, H_2 is one of the desorbed species which appears in two different temperature ranges, the first one between 100 and 300 °C and the second one between 350 and 600 °C (Fig. 12a). It is noteworthy that the desorbed species are in agreement with those observed during HDO experiments in the batch reactor (Fig. 12b). Three TPD peaks are observed which correspond to 3-butene-1,2-diol, 1,3-butadiene and butenes. The most intense and broad peak is that of 1,3-butadiene which appears in a wide temperature range (150–300 and 360–600 °C) implying that the majority of the catalyst surface is covered by it. Similarly, only one desorption peak for butenes is observed which is centered at 250 °C, the same temperature range with that of 1,3-butadiene. On the contrary, 3-butene-1,2-diol appears at two different temperatures zones, with its most intense peak centered between 50 and 100 °C, followed by a second and relatively less intense peak between 200 and 350 °C. The evolution of desorption products with increasing temperature is quite interesting and follows the same trend with the ones observed during HDO experiments. Temperatures below 150 °C, favor the formation of 3-butene-1,2-diol the first HDO product of erythritol (Scheme 1), with its peak being the most dominant one. It can be seen that the desorption of the target olefins, namely 1,3-butadiene and butenes, starts after 150 °C which is very close with the reaction temperature used (140 °C). This indicates that the reaction pathway of erythritol HDO to form 1,3-butadiene is highly dependent on temperature. The appearance of more than one desorption peaks for the same product implies the presence of different type of active sites and/or the same active sites with varying activity[55] as also concluded by CH_3OH-TPSR experiments. Erythritol also remains adsorbed on the catalyst surface, as two desorption peaks are identified, with the first one centered at 160 °C and the second at 400 °C. The corresponding mass for butane was also followed during He-TPD experiments but no peaks were identified in the whole temperature range studied. This can be ascribed to the absence of double bonds in its molecule. In accordance with the TGA profile of the used sample, the He-TPD results can also explain the onset of weight loss observed at low temperatures. Similarly, all the above can further verify the obtained results regarding product distribution. Quantification of the He-TPD results using external standards for butadiene and butenes showed that 0.0057 g_{BD}/g_{cat} (0.57 wt%) and 0.0015 $g_{butenes}/g_{cat}$ (0.15 wt%) remained adsorbed on the catalyst surface after 5 h of testing.

The regenerated catalyst was evaluated under the same reaction conditions and the results are presented in Fig. 13. With respect to the catalyst recovery, the obtained catalyst mass was reduced by 17 %

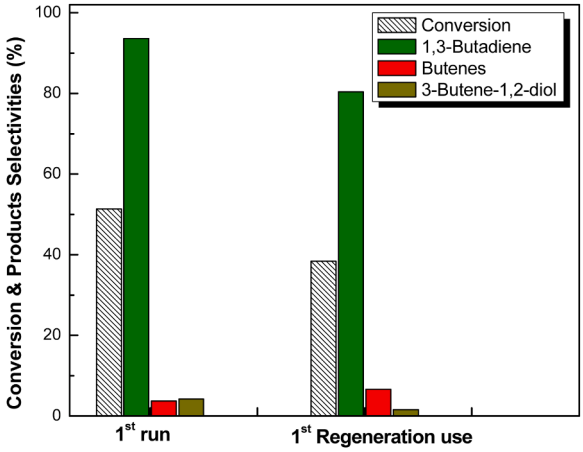

Fig. 13. Reusability test of 5Mo-10Re/CB on erythritol hydrodeoxygenation. (T = 140 °C, $P_{H2,in}$ = 60 bar, catalyst/substrate ratio fresh = 0.56 $g_{cat}/g_{erythritol}$, regenerated = 0.45 $g_{cat}/g_{erythritol}$ and t = 5 h).

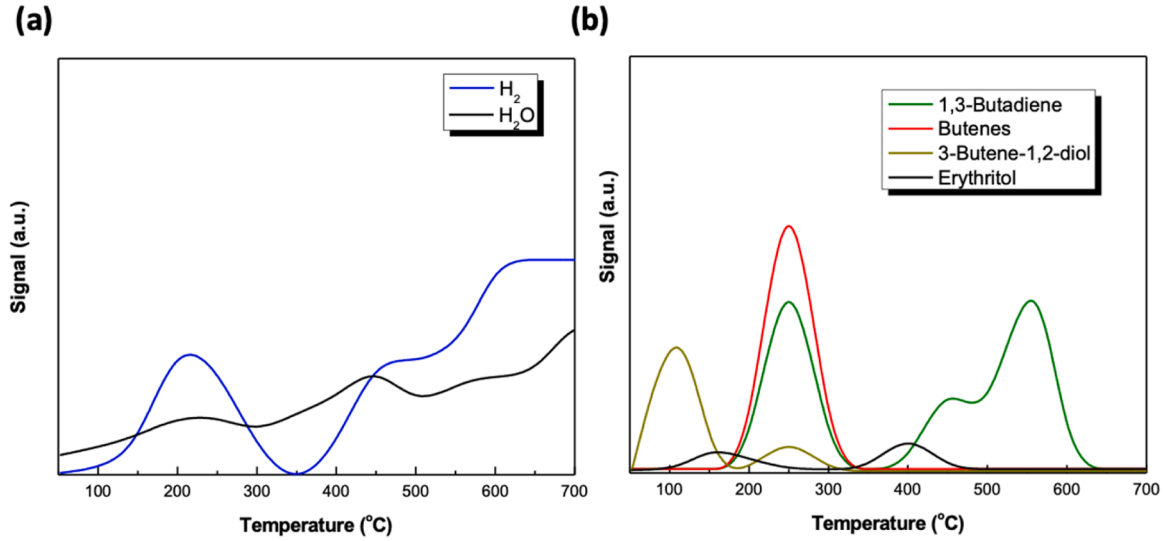

Fig. 12. He-TPD profiles of the used 5Mo-10Re/CB catalyst.

compared to the initial one. It is worthy to observe that erythritol conversion was reduced by 20 %, which is proportional to the lower catalyst amount used implying that leaching of Re species is negligible under the conditions used, as it was also previously mentioned. Comparing now consumption rates (fresh catalyst: 7.41 $mmol_{erythritol}/g_{cat}$, regenerated catalyst: 7.07 $mmol_{erythritol}/g_{cat}$), that of the regenerated catalyst is marginally lower than that of the fresh one indicating that the initial activity was almost fully recovered. The 1,3-butadiene selectivity is reduced by 16 % which might be also correlated to the different catalyst loadings used, while formation of butenes and 3-butene-1,2-diol remains low (< 5 % selectivity). Indeed, the 1,3-butadiene formation rate was reduced by 22 % (fresh catalyst: 6.94 $mmol_{1,3\text{-}BD}/g_{cat}$, regenerated catalyst: 5.45 $mmol_{1,3\text{-}BD}/g_{cat}$).

3.2.7. Effect of solvent

It is known that in both hydrogenolysis and hydrogenation reactions performed in liquid phase the selection of the solvent is of great importance, mostly in hydrogen solubility, as it might be associated with catalyst/reactant/product interactions[56]. In the present study, the effect of different solvents, such as 1,4-dioxane, water and 1-amino-2-propanol on the HDO of erythritol was investigated at 140 °C, 60 bar initial H_2, catalyst/substrate ratio = 0.56 $g_{cat}/g_{erythritol}$ and 5 h. The choice of 1-amino-2-propanol was based on the high solubility of erythritol in contrast to 1,4-dioxane which was the main solvent used in any other case. It should also be noted that blank experiments were performed with 1-amino-2-propanol alone without erythritol in order to avoid falsification the selectivity values of the products. Propylene was the only product detected, however at low selectivity levels (<7 %), while the conversion of the solvent was limited to 6 %. At this point is should also be mentioned that blank experiments in the absence of erythritol were also performed using 1,4-dioxane and the catalyst and the results indicated that under the current reaction conditions the solvent remained fully unconverted. Therefore, all the selectivity values calculated for this reaction originated from erythritol conversion and not from the solvent. The ability of the solvent to be converted might be preferentially attributed to molybdenum, as from previous studies it was found that Mo/CB catalysts can successfully catalyze the HDO reaction of 2-propanol to propylene at low temperatures (< 250 °C)[38,39]. From Fig. 14 it can be easily observed that the selection of solvent has an impact on both conversion and product distribution. By using 1-amino-2-propanol as solvent, adequate selectivity values of 1,3-butadiene equal to 88 % can be achieved, which are close to the ones obtained using 1,4-dioxane (94 %), however, at lower conversion level. On the other hand, with water as solvent, butenes production is favored, along with CO_2 and CH_4 implying that the presence of water enhances erythritol reforming and/or erythritol hydrogenolysis followed by water-gas shift reaction. Water is present in the system as both solvent and product and it seems that it blocks the pores of the catalyst, thus behaving as inhibitor, resulting in lower conversion level[57]. It has been previously reported that the presence of solvent has an impact on the formation of the catalytic active sites in addition to its polarity[58]. Taking into account that solvents such as water, also act as hydrogen donor[59] could explain butenes production instead of 1,3-butadiene due to H_2 excess in the system which enhances the further hydrogenation of the latter. The different solvents used affect hydrogen's solubility, thus altering product distribution. The concentration of H_2 in liquid phase can be estimated according to Henry's law[56,60]. Nonetheless, to calculate hydrogen solubility, the knowledge of Henry's law constant for H_2 in erythritol-solvent mixture is required. The molar fraction of H_2 in the liquid phase was calculated by running a simple simulation in ASPEN Plus Software at the reaction conditions (T = 140 °C, P = 80 bar). The results indicated that the concentration of H_2 in liquid phase was higher in the presence of water as solvent: water $C_{H2,L}$= 0.29 mol/L, 1,4 dioxane $C_{H2,L}$= 0.09 mol/L, and 1-amino-2-propanol: $C_{H2,L}$= 0.07 mol/L) explaining also the differences in product distribution. It is also interesting to observe that hydrogen's concentration values are very close with the use of 1,4-dioxane and 1-amino-2-propanol justifying the similar catalytic activity.

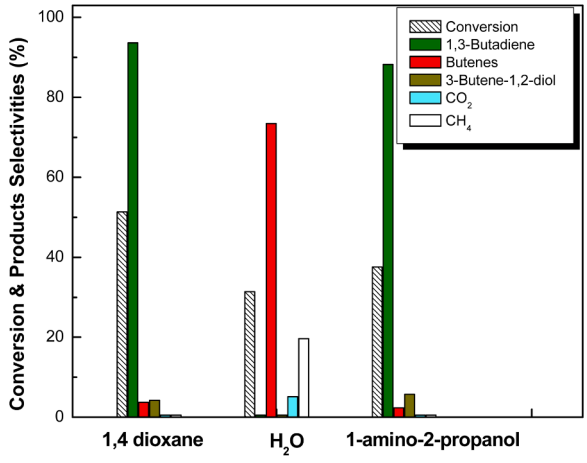

Fig. 14. Effect of solvent on erythritol conversion and product distribution over 5Mo-10Re/CB. (T = 140 °C, $P_{in,H2}$ = 60 bar, catalyst/substrate ratio = 0.56 $g_{cat}/g_{erythritol}$ and t = 5 h).

3.2.8. Effect of synthesis parameters

As the mixed 5Mo-10Re/CB catalyst showed the most promising performance in erythritol HDO, the effects of calcination atmosphere, as well as metal loading under oxidizing atmosphere were explored at reaction conditions under which the maximum 1,3-butadiene selectivity was achieved (T = 140 °C, $P_{H2,in}$ = 60 bar, catalyst/substrate = 0.56 $g_{cat}/g_{erythritol}$ and t = 5 h). The results are summarized in Table 6 and it seems that the calcination atmosphere considerably affects product distribution, while it has a minor effect on erythritol conversion. Comparing entry 1 with entry 2, it is obvious that the 5Mo-10Re/CB_{OXID} catalyst calcined under air favors C=C hydrogenation as butane is the main product detected in gas phase with 60 % selectivity followed by butenes (26 %). This can be attributed to different crystal structures of the catalysts as determined by XRD analysis. Under an oxidizing calcination atmosphere (Fig. 15) the diffraction peaks of Mo-Re/CB_{OXID} catalysts become broader and less intense indicating a decrease in crystallinity which resembles the appearance of an amorphous material. This transformation in the structure might be the reason that affects the catalytic activity. The two diffraction peaks detected at 2θ = 24.91 and 2θ = 43.31 correspond to that of the support. According to XPS results mentioned below, fully oxidized species are observed on the surface implying that they are not the appropriate active phase for the reaction to proceed towards the target product. The presence of both oxidized and reduced molybdenum-rhenium species (Fig. 2) seems to be an important precondition for efficient 1,3-butadiene production. It is also interesting to observe that XRD patterns of used materials are the same with that of the fresh ones in every case and under any calcination treatment, indicating that under the applied reaction conditions catalyst sintering or further reduction is negligible.

Considering the above results, along with those of the CH_3OH-TPSR experiments, oxidized and partially reduced molybdenum and rhenium species are most likely the active species that drive erythritol HDO to 1,3-butadiene. To further confirm this assumption, XPS measurements of fresh 5Re/CB, 5Mo-10Re/CB and 5Mo-10Re/CB_{OXID}, as well as of used 5Mo-10Re/CB were performed to obtain more information regarding the composition and the oxidation state of the metal species appearing in the upper surface layers. Fig. 16 visualizes the Mo 3d XPS spectrum of 5Mo-10Re/CB, 5Mo-10Re/CB_{OXID} and used 5Mo-10Re/CB, while Fig. 17 shows the Re 4 f spectrum of the above-mentioned catalytic materials including 5Re/CB. According to literature data, the typical values that correspond to each oxidation state of both Mo 3d and

Table 6
Catalytic performance over mixed Mo-Re/CB catalysts calcined under different atmospheres (N_2 or air) (T = 140 °C, $P_{in,H2}$ = 60 bar, catalyst/substrate ratio = 0.56 $g_{cat}/g_{erythritol}$ and t = 5 h).

			Product selectivities (%)						
Entry	Catalyst	Conversion (%)	1,3-Butadiene	Butenes	Butane	3-Butene−1,2-diol	Butanediols	Erythritol isomers	Others*
1	5Mo−10Re/CB	51	93	4	-	4	0.2	-	
2	5Mo−10Re/CB_{OXID}	57	-	26	60	1	1	5	3

* Others: CO_2 – CH_4 – C_2H_6 – C_3H_8.

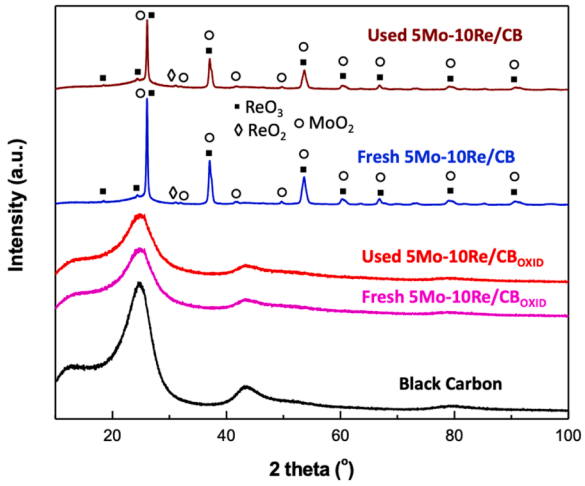

Fig. 15. XRD patterns of fresh and used Mo-Re/CB catalysts calcined under oxidizing atmosphere and used Mo-Re/CB calcined under inert (N_2) atmosphere.

Re 4 f are presented in Table 7. For both fresh 5Mo-10Re/CB and 5Mo-10Re/CB_{OXID}, molybdenum species in the highest oxidation state (Mo^{6+}) are the most abundant species indicating that calcination conditions (inert or oxidizing) do not affect the upper surface layers of the catalyst in contrast to bulk species (according to XRD results, Fig. 14). In addition to obtaining a different structure between the bulk and the upper surface layer of the catalyst, the fact that MoO_3 species were not identified by XRD might also imply that they are highly dispersed on the support and/or that they are amorphous.

Another remarkable difference between 5Mo-10Re/CB and 5Mo-10Re/CB_{OXID} is the observed binding energy of the Mo 4p level in the Re4f spectrum of the latter. The Mo4p spectrum is distinct only in the 4 f spectrum and it occurs because of the splitting of the final state of $4p^6 4d^n$[61].

In the used 5Mo-10Re/CB sample, a relatively low amount of Mo^{4+} is formed as shown by the peaks located at 228.86 and 231.66 eV, implying that the presence of high hydrogen pressure during experiments slightly promotes the reduction of Mo^{6+} species to Mo^{4+}, the latter not exceeding 4 % on atomic basis. The Re 4 f spectrum of all catalytic materials presents a few clear differences in the nature of rhenium species on the upper surface layers, with their population significantly varying in each case. From Fig. 16 it is clear that different oxidation states of rhenium coexist on the surface, with that of partially reduced (Re^{6+}) being the most predominant ones. However, it seems that the oxide, even in fresh samples, is partially reduced, giving rise to Re^{4+} species, suggesting that the applied calcination conditions under N_2 atmosphere favors the reducibility of rhenium in accordance with the XRD results previously mentioned. This trend is not observed for 5Mo-10Re/CB $_{OXID}$, where only the oxidized species are identified. Comparing fresh 5Mo-10Re/CB with used 5Mo-10Re/CB, the population of Re^{6+} species is decreased at half, from 86.2 % to 44.1 %, while that of Re^{4+} considerably increases from 7.8 % to 27.1 %. It is also interesting to observe that the concentration of fully oxidized Re^{7+} species is highly increased from 6.1 in the fresh sample to 28.7 in the used. These reduction and oxidation changes of Re valence on the catalyst surface indicates most likely a reverse Mars van Krevelen mechanism in agreement with glycerol HDO over molybdenum catalysts [36,62]. However, it should be noted that the XPS measurements were conducted ex-situ, also affecting the oxidation state of the surface rhenium species. However, as the same procedure was applied for all measurements, the extent of oxidation by the exposure to air might be similar to all fresh and used samples. Comparing now the catalytic data with both CH_3OH-TPSR and XPS results, it can be suggested that the selective HDO of erythritol to butadiene is attributed to the high valent Re species (Re^{7}+, Re^{6+}) and partially reduced rhenium species (Re^{4+}) with the fully oxidized molybdenum ones (Mo^{6+}).

4. Conclusions

In this study the activity of supported rhenium and molybdenum metal oxides in erythritol HDO to 1,3-butadiene was evaluated in liquid phase under batch conditions employing high hydrogen pressure (60 bar) and low temperature (140 °C). Catalysts supported on carbon

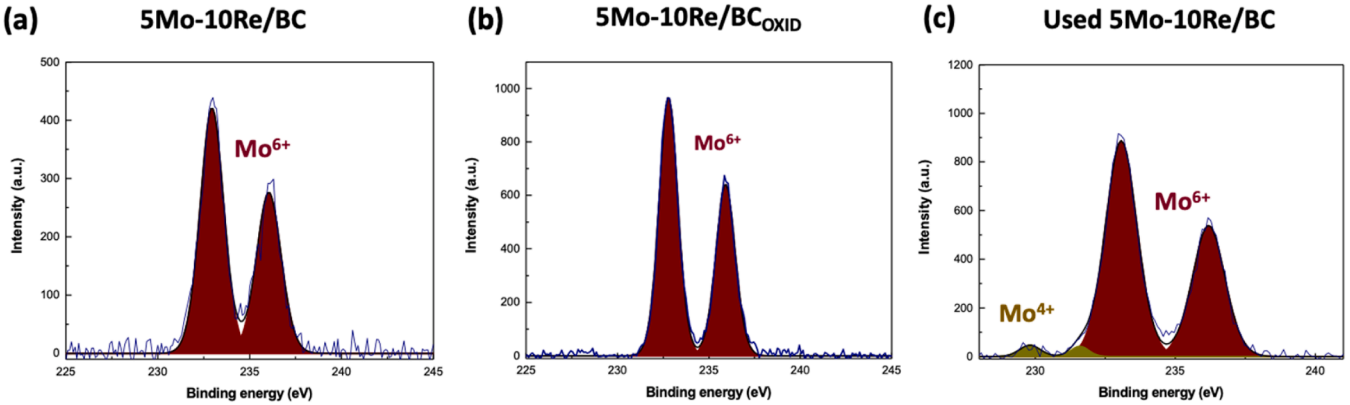

Fig. 16. XPS Mo 3d spectra (black line) and the fitted (blue line) for (a) 5Mo-10Re/CB, (b) 5Mo-10Re/CB_{OXID} and (c) used 5Mo-10Re/CB.

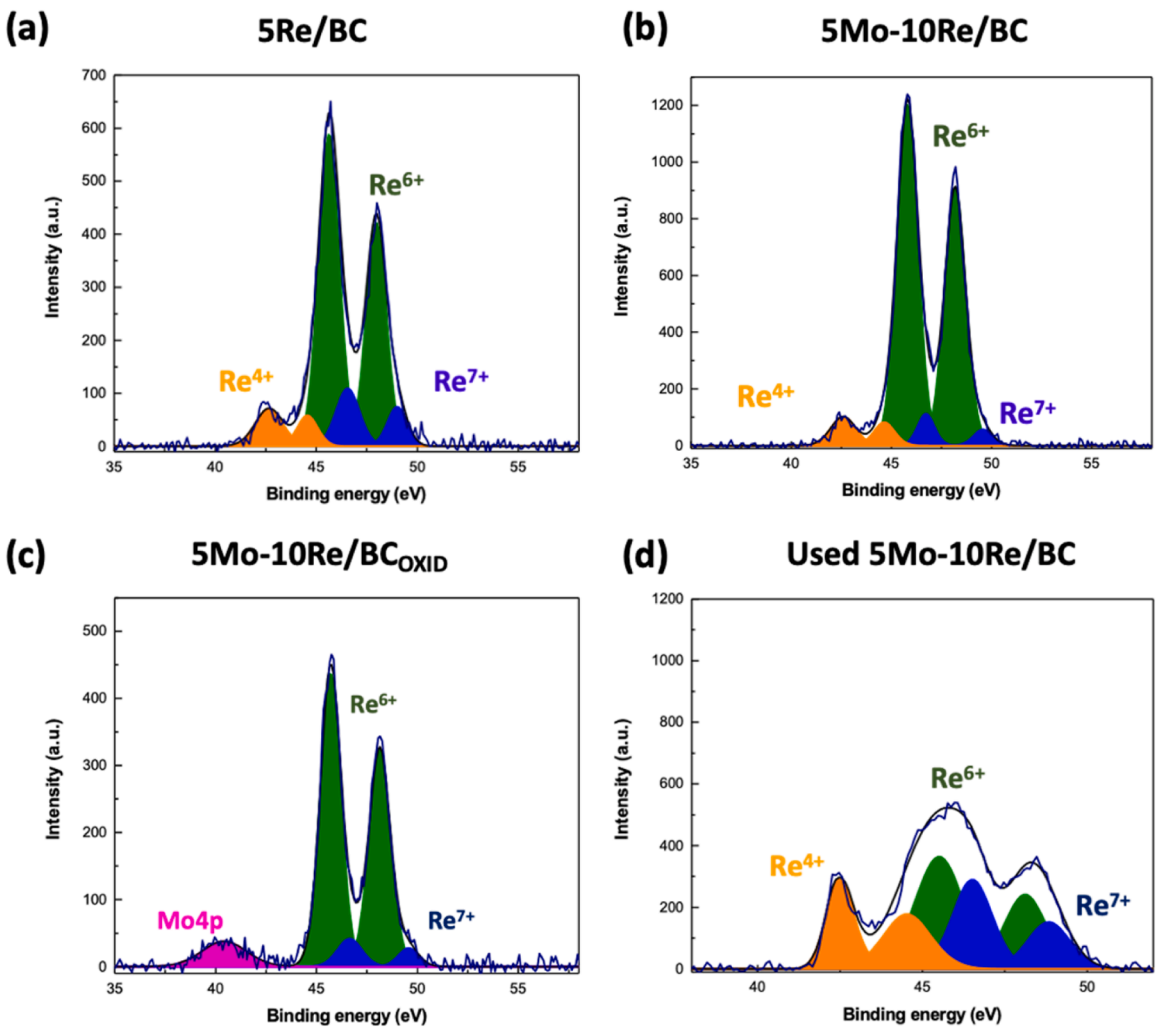

Fig. 17. XPS Re 4 f spectra (black line) and the fitted (blue line) for (a) 5Re/CB, (b) 5Mo-10Re/CB, (c) 5Mo-10Re/CB_{OXID} and (d) used 5Mo-10Re/CB.

Table 7
XPS quantification data for population of Mo and Re at different oxidation states and XPS standard binding energies (eV) of Mo 3d and Re 4 f levels for different oxidation states of molybdenum and rhenium [63–67].

Population of oxidation state of catalytic materials (%)					Standard reported values (eV)			
Oxidation state	5Re/CB	5Mo−10Re/CB	5Mo−10Re/CB_{OXID}	used 5Mo−10Re/CB	Mo 3d5/2	Mo 3d3/2	Re 4f7/2	Re 4f5/2
Mo^{6+}	100	100	96.40	232.5	235.7			
Mo^{4+}				3.70	230.1	232.2		
Re^{7+}	14.60	6.10	9.11	28.80			45.4	47.8
Re^{6+}	73.90	86.20	90.89	44.10			42.9	45.3
Re^{4+}	11.50	7.80		27.10			42.7	45.1

black with low rhenium loadings 2–5 wt%, showed moderate activity but more importantly the selectivity to 1,3-butadiene was low because of further hydrogenation to butenes. A rhenium-enriched catalyst (20 wt % loading) highly favored 1,3-butadiene production (88 % selectivity) accompanied by the highest erythritol conversion equal to 65 %. The subsequent impregnation of molybdenum with rhenium on carbon black resulted in highly active materials which favored 1,3-butadiene production. It was found that 3-butene-1,2-diol is the main intermediate towards 1,3-butadiene, as its production was highly favored at short reaction times, whereas extended reaction times (> 5 h) promoted the further conversion of the target product to butenes and/or butane. Experimental results indicated that increased temperature, H_2 pressure and catalyst loading enhanced both conversion and 1,3-butadiene production. Under the optimum reaction conditions (T = 140 °C, $P_{in,H2}$ = 60 bar, catalyst/substrate ratio = 0.56, $g_{cat}/g_{erythritol}$ and t = 5 h) and over 5Mo-10Re/CB the highest 1,3-butadiene selectivity of 93 % is achieved at 51 % erythritol conversion. Catalyst reusability was also evaluated after regeneration of the used catalyst by N_2 treatment. Both activity and selectivity to 1,3-butadiene did not show any significant differences implying that the catalyst active sites were fully recovered after regeneration treatment.

The synthesis procedure parameters, such as calcination conditions, have an important impact on conversion and product selectivity. More specifically, calcination under air flow and low temperatures (300 °C), led to an amorphous catalyst structure promoting mostly butane formation instead of 1,3-butadiene which was the main product obtained when the calcination process was performed under inert atmosphere (N_2) and high temperature (500 °C). XPS measurements of the used

5Mo-10Re/CB catalyst indicated the presence of fully oxidized molybdenum (Mo^{6+}) species coexisting with fully oxidized Re^{7+} and partially reduced (Re^{6+}, Re^{4+}) rhenium species which most likely are the active sites that promote the selective formation of 1,3-butadiene from erythritol. CH_3OH-TPSR results suggested that both acid and redox sites coexist on the catalyst surface, with redox sites being the most dominant ones over 5Mo-10Re/CB catalyst enhancing erythritol HDO to 1,3-butadiene.

Although in this study a 48 % yield was achieved, which is lower compared to one previously mentioned [33], it is considered very promising as it is attained within a significantly shorter reaction time and lower catalyst/substrate ratio (current study: 5 h and catalyst/substrate = 0.56 $g_{cat}/g_{erythritol}$, report in the literature [33]: 20 h and catalyst/substrate = 1.2 $g_{cat}/g_{erythritol}$). This also leads to higher productivity values (current study: 0.075 $g_{1,3\text{-}BD}/g_{cat}h$, report in the literature: 0.036 $g_{1,3\text{-}BD}/g_{cat}h$) which can further improve the viability of the process. The current encouraging results shed lights on using mixed Mo-Re catalysts supported on carbon black reaching high 1,3-butadiene yields. Nonetheless, further studies are required to fully comprehend the various phenomena occurred in this reaction and thus, these results can lay down the groundwork for further studies of erythritol HDO under continuous flow conditions as they are mostly preferred for industrial applications.

CRediT authorship contribution statement

Georgia Ioannidou: Conceptualization, Methodology, Software, Validation, Data curation, Formal analysis, Investigation, Visualization, Writing – Original draft. **Marius Drexler:** Methodology, Software, Validation, Formal analysis, Writing - review & editing. **Ulrich Arnold:** Methodology, Software, Validation, Formal analysis, Supervision, Writing - review & editing. **Joerg Sauer:** Validation, Supervision, Resources, Project administration, Funding acquisition, Writing - review & editing. **Angeliki Lemonidou:** Conceptualization, Methodology, Validation, Supervision, Resources, Project administration, Funding acquisition, Writing - review & editing.

Declaration of Competing Interest

The authors declare no competing financial interest.

Acknowledgments

Ms. Georgia Ioannidou acknowledges the Helmholtz Association of German Research Centers for the doctoral scholarship through the European program Helmholtz European Partnership for Technological Advancements (HEPTA). The authors would like to acknowledge Ms. Birgit Rolli from Institute of Catalysis Research and Technology (IKFT) at Karlsruhe Institute of Technology (KIT) for the support with GC measurements, as well as Mr. Dimitrios Karfaridis from the Physics Department of Aristotle University of Thessaloniki for the XPS measurements.

Data Availability

Data will be made available on request.

References

[1] A.A. Kiss, R. Smith, Energy 203 (2020) 117788, https://doi.org/10.1016/j.energy.2020.117788.
[2] P.E. Brockway, A. Owen, L.I. Brand-Correa, L. Hardt, Nat. Energy 4 (2019) 612–621, https://doi.org/10.1038/s41560-019-0425-z.
[3] M.A. Siddik, M.T. Islam, A.K.M.M. Zaman, M.M. Hasan, Int. J. Energy Environ. Econ. 28 (2021) 103–118.
[4] P. Gabrielli, L. Rosa, M. Gazzani, R. Meys, A. Bardow, M. Mazzotti, G. Sansavini, One Earth 6 (2023) 682–704, https://doi.org/10.1016/j.oneear.2023.05.006.
[5] M. Flores-Granobles, M. Saeys, Green. Chem. 25 (2023) 6459–6471, https://doi.org/10.1039/d3gc01237a.
[6] V. Zacharopoulou, A.A. Lemonidou, Catalysts 8 (2018) 2–20, https://doi.org/10.3390/catal8010002.
[7] S.A. Chernyak, M. Corda, J.P. Dath, V.V. Ordomsky, A.Y. Khodakov, Chem. Soc. Rev. 51 (2022) 7994–8044, https://doi.org/10.1039/d1cs01036k.
[8] H. Duan, Y. Yamada, S. Sato, Appl. Catal. A Gen. 491 (2015) 163–169, https://doi.org/10.1016/j.apcata.2014.12.006.
[9] C.E. Cabrera Camacho, A.L. Villanueva Perales, B. Alonso-Fariñas, F. Vidal-Barrero, P. Ollero, J. Clean. Prod. 374 (2022) 133963, https://doi.org/10.1016/j.jclepro.2022.133963.
[10] C. Brencio, M. Maruzzi, G. Manzolini, F. Gallucci, Int. J. Hydrog. Energy 47 (2022) 21375–21390, https://doi.org/10.1016/j.ijhydene.2022.04.259.
[11] G. Tanimu, O. Elmutasim, H. Alasiri, K. Polychronopoulou, Chem. Eng. Sci. 280 (2023), https://doi.org/10.1016/j.ces.2023.119059.
[12] A. Bohre, A. Modak, V. Chourasia, P. Ram Jadhao, K. Sharma, K. Kishore Pant, Chem. Eng. J. 450 (2022) 138032, https://doi.org/10.1016/j.cej.2022.138032.
[13] P. Sudarsanam, N.K. Gupta, B. Mallesham, N. Singh, P.N. Kalbande, B.M. Reddy, B. F. Sels, ACS Catal. 11 (2021) 13603–13648, https://doi.org/10.1021/acscatal.1c03326.
[14] A. Hommes, H.J. Heeres, J. Yue, ChemCatChem 11 (2019) 4671–4708, https://doi.org/10.1002/cctc.201900807.
[15] B. Biswas, N. Pandey, Y. Bisht, R. Singh, J. Kumar, T. Bhaskar, Bioresour. Technol. 237 (2017) 57–63, https://doi.org/10.1016/j.biortech.2017.02.046.
[16] Y. Weng, T. Wang, P. Duan, C. Wang, F. Wang, Q. Liu, L. Chen, H. Wang, Z. Liang, L. Ma, Energy Technol. 6 (2018) 1763–1770, https://doi.org/10.1002/ente.201700885.
[17] X. Jin, J. Shen, W. Yan, M. Zhao, P.S. Thapa, B. Subramaniam, R.V. Chaudhari, ACS Catal. 5 (2015) 6545–6558, https://doi.org/10.1021/acscatal.5b01324.
[18] C. Xu, E. Paone, D. Rodríguez-Padrón, R. Luque, F. Mauriello, Renew. Sustain. Energy Rev. 127 (2020) 109852, https://doi.org/10.1016/j.rser.2020.109852.
[19] S. De, B. Saha, R. Luque, Bioresour. Technol. 178 (2015) 108–118, https://doi.org/10.1016/j.biortech.2014.09.065.
[20] S. Kim, E.E. Kwon, Y.T. Kim, S. Jung, H.J. Kim, G.W. Huber, J. Lee, Green. Chem. 21 (2019) 3715–3743, https://doi.org/10.1039/c9gc01210a.
[21] W. Wang, T. Tago, H. Fujitsuka, Catal. Today 411 (2022) 113827, https://doi.org/10.1016/j.cattod.2022.06.042.
[22] J.H. Jang, H. Sohn, J. Camacho-Bunquin, D. Yang, C.Y. Park, M. Delferro, M. M. Abu-Omar, ACS Sustain. Chem. Eng. 7 (2019) 11438–11447, https://doi.org/10.1021/acssuschemeng.9b01253.
[23] S. Tazawa, N. Ota, M. Tamura, Y. Nakagawa, K. Okumura, K. Tomishige, ACS Catal. 6 (2016) 6393–6397, https://doi.org/10.1021/acscatal.6b01864.
[24] M. Grilc, B. Likozar, J. Levec, Appl. Catal. B 150–151 (2014) 275–287, https://doi.org/10.1016/j.apcatb.2013.12.030.
[25] M. Grilc, G. Veryasov, B. Likozar, A. Jesih, J. Levec, Appl. Catal. B 163 (2015) 467–477, https://doi.org/10.1016/j.apcatb.2014.08.032.
[26] D.A. Rzechonek, A. Dobrowolski, W. Rymowicz, A.M. Mirończuk, Crit. Rev. Biotechnol. 38 (2018) 620–633, https://doi.org/10.1080/07388551.2017.1380598.
[27] W.O. Bernt, J.F. Borzelleca, G. Flamm, I.C. Munro, RTP 24 (2) (1996) S191–S197, https://doi.org/10.1006/rtph.1996.0098.
[28] Y. Nakagawa, T. Kasumi, J. Ogihara, M. Tamura, T. Arai, K. Tomishige, ACS Omega 5 (2020) 2520–2530, https://doi.org/10.1021/acsomega.9b04046.
[29] M. Stalpaert, K. Janssens, C. Marquez, M. Henrion, A.L. Bugaev, A.V. Soldatov, D. De Vos. ACS Catal. 10, (202) 9401-9409. https://doi.org/10.1021/acscatal.0c02188.
[30] M. Gu, L. Liu, Y. Nakagawa, C. Li, M. Tamura, Z. Shen, X. Zhou, Y. Zhang, K. Tomishige, ChemSusChem 14 (2021) 642–654, https://doi.org/10.1002/cssc.202002357.
[31] M. Shiramizu, F.D. Toste, Angew. Chem. 51 (2012) 8082–8086, https://doi.org/10.1002/anie.201203877.
[32] J. Li, M. Lutz, M. Otte, R.J.M. Klein Gebbink, ChemCatChem 10 (2018) 4755–4760, https://doi.org/10.1002/cctc.201801151.
[33] K. Yamaguchi, J. Cao, M. Betchaku, Y. Nakagawa, M. Tamura, A. Nakayama, M. Yabushita, K. Tomishige, ChemSusChem 15 (2022) e202102663, https://doi.org/10.1002/cssc.202102663.
[34] N. Ota, M. Tamura, Y. Nakagawa, K. Okumura, K. Tomishige, ACS Catal. 6 (2016) 3213–3226, https://doi.org/10.1021/acscatal.6b00491.
[35] J. Cao, S. Larasati, M. Yabushita, Y. Nakagawa, J. Wärnå, D.Y. Murzin, D. Asada, A. Nakayama, K. Tomishige, ACS Catal. 14 (2024) 1663–1677, https://doi.org/10.1021/acscatal.3c04785.
[36] V. Zacharopoulou, E.S. Vasiliadou, A.A. Lemonidou, ChemSusChem 11 (2018) 264–275, https://doi.org/10.1002/cssc.201701605.
[37] V. Zacharopoulou, E.S. Vasiliadou, A.A. Lemonidou, Green. Chem. 17 (2015) 903–912, https://doi.org/10.1039/c4gc01307g.
[38] G. Ioannidou, A. Lemonidou, Green. Chem. (2023) 10043–10060, https://doi.org/10.1039/D3GC02902F.
[39] G. Ioannidou, V.– L. Yfanti, A.A. Lemonidou, Catal. Today 423 (2023) 113902, https://doi.org/10.1016/j.cattod.2022.09.008.
[40] R. Phillips, K. Jolley, Y. Zhou, R. Smith, Carbon Trends 5 (2021) 100124, https://doi.org/10.1016/j.cartre.2021.100124.
[41] C. Herrera, I.T. Ghampson, K. Cruces, C. Sepúlveda, L. Barrientos, D. Laurenti, C. Geantet, R. Serpell, D. Contreras, V. Melin, N. Escalona, Fuel 259 (2020) 116245, https://doi.org/10.1016/j.fuel.2019.116245.
[42] I.T. Ghampson, G. Pecchi, J.L.G. Fierro, A. Videla, N. Escalona, Appl. Catal. B 208 (2017) 60–74, https://doi.org/10.1016/j.apcatb.2017.02.047.

[43] M.L. Gothe, K.L.C. Silva, A.L. Figueredo, J.L. Fiorio, J. Rozendo, B. Manduca, V. Simizu, R.S. Freire, M.A.S. Garcia, P. Vidinha, Eur. J. Inorg. Chem. 2021 (2021) 4043–4065, https://doi.org/10.1002/ejic.202100459.
[44] M. Badlani, I.E. Wachs, Catal. Lett. 75 (2001) 137–149, https://doi.org/10.1023/A:1016715520904.
[45] X. Wang, I.E. Wachs, Catal. Today 96 (2004) 211–222, https://doi.org/10.1016/j.cattod.2004.06.145.
[46] L.E. Briand, J.M. Jehng, L. Cornaglia, A.M. Hirt, I.E. Wachs, Catal. Today 78 (2003) 257–268, https://doi.org/10.1016/S0920-5861(02)00350-4.
[47] Z. Skoufa, E. Heracleous, A.A. Lemonidou, J. Catal. 322 (2015) 118–129, https://doi.org/10.1016/j.jcat.2014.11.014.
[48] G. Garcia Cortez, J.L.G. Fierro, M.A. Bañares, Catal. Today 78 (2003) 219–228, https://doi.org/10.1016/S0920-5861(02)00341-3.
[49] T. Feng, J.M. Vohs, J. Catal. 208 (2002) 301–309, https://doi.org/10.1006/jcat.2002.3587.
[50] W. Zhao, B. Zhang, G. Wang, H. Guo, J. Energy Chem. 23 (2014) 201–206, https://doi.org/10.1016/S2095-4956(14)60136-4.
[51] P. Yan, M.M.J. Li, E. Kennedy, A. Adesina, G. Zhao, A. Setiawan, M. Stockenhuber, Catal. Sci. Technol. 10 (2020) 810–825, https://doi.org/10.1039/C9CY01970G.
[52] F.M. Harth, B. Likozar, M. Grilc, Mater. Today Chem. 26 (2022), https://doi.org/10.1016/j.mtchem.2022.101191.
[53] E.M. Virgilio, M.E. Sad, C.L. Padró, Appl. Catal. A Gen. 643 (2022) 118691, https://doi.org/10.1016/j.apcata.2022.118691.
[54] M. Arrais Gonçalves, E. Karine Lourenço Mares, J. Roberto Zamian, G. Narciso da Rocha Filho, L. Rafael Vieira da Conceição, Fuel 304 (2021) 121463, https://doi.org/10.1016/j.fuel.2021.121463.
[55] X. Wang, F. Zhao, L. Huang, Catalysts 10 (2020), https://doi.org/10.3390/catal10010043.
[56] E.S. Vasiliadou, A.A. Lemonidou, Chem. Eng. J. 231 (2013) 103–112, https://doi.org/10.1016/j.cej.2013.06.096.
[57] R. Gholami, M. Alyani, K.J. Smith, Catalysts 5 (2015) 561–594, https://doi.org/10.3390/catal5020561.
[58] G. Dodekatos, J. Ternieden, S. Schünemann, C. Weidenthaler, H. Tüysüz, Catal. Sci. Technol. 8 (2018) 4891–4899, https://doi.org/10.1039/c8cy01284a.
[59] Y.K. Park, J.M. Ha, S. Oh, J. Lee, Chem. Eng. J. 404 (2021) 126527, https://doi.org/10.1016/j.cej.2020.126527.
[60] M. Décultot, A. Ledoux, M.C. Fournier-Salaün, L. Estel, J. Chem. Thermodyn. 138 (2019) 67–77, https://doi.org/10.1016/j.jct.2019.05.003.
[61] N. Kumar, A.T. Kozakov, A.V. Nezhdanov, R.M. Smertin, V.N. Polkovnikov, N. I. Chkhalo, A.I. Mashin, A.N. Nikolskii, A.A. Scrjabin, S.Y. Zuev, J. Phys. Chem. C. 124 (2020) 17795–17805, https://doi.org/10.1021/acs.jpcc.0c03904.
[62] A.V. Mironenko, D.G. Vlachos, J. Am. Chem. Soc. 138 (2016) 8104–8113, https://doi.org/10.1021/jacs.6b02871.
[63] E. Blanco, P. Cabeza, V. Naharro Ovejero, C. Contreras, A.B. Dongil, I. T. Ghampson, N. Escalona, Catal. Today 420 (2023) 11403, https://doi.org/10.1016/j.cattod.2023.02.008.
[64] X. Liu, J. Zhou, Z. Jiang, Z. Huang, B. Li, Z. Ma, Y. Yang, Y. Huang, Y. Zhang, V. D. Botcha, R.J. Chung, J. Liang, X. Li, Y. Li, W. He, Adv. Electron Mater. 10 (2023) 2300711, https://doi.org/10.1002/aelm.202300711.
[65] P. Krukowski, M. Piskorski, M. Rogala, P. Dabrowski, I. Lutsyk, W. Kozlowski, D. A. Kowalczyk, P. Krempinski, M. Le Ster, A. Nadolska, K. Toczekt, P. Przybysz, R. Dunal, W. Rys, S. Sarkar, B. Luszczynska, P.J. Kowalczyk, Opto-Electron. Rev. 32 (2023) e148441, https://doi.org/10.24425/opelre.2024.148441.
[66] M. Alda-Onggar, P. Mäki-Arvela, K. Eränen, A. Aho, J. Hemming, P. Paturi, M. Peurla, M. Lindblad, I.L. Simakova, D.Y. Murzin, ACS Sustain. Chem. Eng. 6 (2018) 16205–16218, https://doi.org/10.1021/acssuschemeng.8b03035.
[67] J. Okal, W. Tylus, L. Kępiński, J. Catal. 225 (2004) 498–509, https://doi.org/10.1016/j.jcat.2004.05.004.